A DESSERTATION

FOR THE DEGREE OF DOCTOR OF PHILOSOPHY

Anti-tumor Effects of Canine and Human Adipose Tissue-derived Mesenchymal Stem Cells in a Xenograft Mouse Model for Melanoma

흑색종 이종이식 마우스모델에서 개와 사람의 지방유래 중간엽줄기세포의 항암효과

By

Jin-Ok Ahn

VETERINARY INTERNAL MEDICINE

DEPARTMENT OF VETERINARY MEDICINE

GRADUATE SCHOOL

SEOUL NATIONAL UNIVERSITY

2015.02.

Anti-tumor Effects of Canine and Human Adipose Tissue-derived Mesenchymal Stem Cells in a Xenograft Mouse Model for Melanoma

By

Jin-Ok Ahn

A Dissertation submitted to
the Graduate School of Seoul National University
in partial fulfillment of the requirement
for the degree of Doctor of Philosophy
in Veterinary Medicine

Supervised by
Professor Hwa-Young Youn

November, 2014

Veterinary Internal Medicine
Department of Veterinary Medicine
Graduate School
Seoul National University

December, 2014

Anti-tumor Effects of Canine and Human Adipose Tissue-derived Mesenchymal Stem Cells in a Xenograft Mouse Model for Melanoma

흑색종 이종이식 마우스모델에서 개와 사람의 지방유래 중간엽줄기세포의 항암효과

지도교수 윤 화 영

이 논문을 수의학 박사 학위 논문으로 제출함

2014 년 11 월

서울대학교 대학원

수의학과 수의내과학 전공

안 진 옥

안진옥의 박사 학위논문을 인준함

2014 년 12 월

위 원 장 신 남 식 (인)

부위원장 윤 화 영 (인)

위 원 김 용 백 (인)

위 원 이 희 우 (인)

위 원 서 경 원 (인)

Anti-tumor Effects of Canine and Human Adipose Tissue-derived Mesenchymal Stem Cells in a Xenograft Mouse Model for Melanoma

Jin-Ok Ahn

(Supervised by Prof. Hwa-Young Youn)

Veterinary Internal Medicine

Department of Veterinary Medicine

Graduate School

Seoul National University

Abstract

Mesenchymal stem cells (MSCs) show promising potential for use in regenerative medicine and a variety of diseases because of their capacity of self-renewal and multipotential differentiation. Especially, MSCs have been identified as promising therapeutic tools in cancer treatment since they possess a powerful capacity for tumor-directed migration and incorporation, highlighting their potential as an optimal vehicle for delivering anticancer agents.

This dissertation is composed of two parts. The first part of the study was performed to investigate the anti-tumor effect of human adipose tissue-derived mesenchymal stem cells (AT-MSCs) on human melanoma. The growth-inhibitory effect of AT-MSC-conditioned medium (AT-MSC-CM) on A375SM and A375P melanoma cells was evaluated using a cell viability assay. The results showed that AT-MSC-CM significantly inhibited the viability of A375SM and A375P cells. To investigate whether AT-MSC-CM inhibit melanoma cell proliferation by altering cell cycle distribution and inducing apoptosis, A375SM and A375P cells were analyzed by flow cytometry after treatment with AT-MSC-CM for 72 h. AT-MSC-CM induced G_0/G_1 cell cycle arrest and apoptosis in A375SM and A375P melanoma cells. Western blot assays showed that cyclin D1 levels were decreased and caspase-3, caspase-7 and PARP protein levels were increased in melanoma cells cultured with AT-MSC-CM. To evaluate an anti-tumor effect of AT-MSCs on melanoma *in vivo*, CM-DiI-labeled AT-MSCs were circumtumorally injected to the tumor-bearing nude mice, and change in the tumor size was monitored. Treatment with AT-MSCs suppressed tumor growth in the mice and fluorescence analysis revealed that AT-MSCs migrated efficiently to the tumor tissues.

The second part of the dissertation was designed to test the hypothesis that the stem cell-based gene therapy combined with low-dose cisplatin would improve therapeutic efficacy against canine melanoma. The IFN-β

transduced canine AT-MSCs (cAT-MSC-IFN-β) inhibited the growth of LMeC canine melanoma cells *in vitro* in direct as well as indirect co-culture systems. Flow cytometric cell cycle analysis showed that the proportion G_0/G_1 phase LMeC cells co-cultured with cAT-MSC-IFN-β was higher than that of the controls. G1 arrest occurred concurrently with a reduction in the percentage of S phase cells. In animal experiments using BALB/c nude mouse xenograft model which was established by injecting LMeC cells subcutaneously, the combined treatment of cAT-MSC-IFN-β and low-dose cisplatin significantly reduced tumor volume compared to the control and single agent treatment groups. Fluorescent microscopic analysis of the tumor section provided evidence for homing of cAT-MSC-IFN-β to the tumor site and TUNEL (terminal deoxynucleotidyl transferase-mediated nick-end labeling) assay showed that the combination treatment of cAT-MSC-IFN-β and low-dose cisplatin induced high levels of cell apoptosis.

In conclusion, cell therapy using AT-MSCs demonstrated an anti-tumor effect on canine and human melanomas, suggesting a possible therapeutic option for this type of cancer. These findings may provide valuable information warranting further explorations of the application of the combined therapy for various tumors including malignant melanoma.

Keywords : dog, cancer cell therapy, interferon beta, human, melanoma, adipose tissue-derived mesenchymal stem cells (AT-MSCs)

Student Number **: 2011-30491**

Content

CHAPTER III.

Anti-tumor effect of adipose tissue-derived mesenchymal stem cells expressing interferon-β and treatment with cisplatin in a xenograft mouse model for canine melanoma

Abbreviations

Asc 2P	L-ascorbic acid 2-phosphate
AT-MSC-CM	Adipose tissue-derived mesenchymal stem cell-conditioned medium
AT-MSC-Mock	Empty vector-transduced AT-MSC
AT-MSCs	Adipose tissue-derived mesenchymal stem cells
BM-MSCs	Bone marrow-derived mesenchymal stem cells
bp	Base pair
BPE	Bovine pituitary extract
CD	Cluster of differentiation protein
Cdks	Cyclin-dependent kinases
CKI	Cyclin-dependent kinases inhibitor
CO_2	Carbon dioxide
CXCR	CXC chemokine receptor
Dkk	Dickkopf-related protein
DMEM	Dulbecco's modified Eagle medium
DNA	Deoxyribonucleic acid

EDTA	Ethylenediamine tetraacetic acid
EGF	Epidermal growth factor
ELISA	Enzyme-linked immunosorbent assay
FACS	Flow cytometry assisted cell sorting
FADD	Fas-associated protein with death domain
FBS	Fetal bovine serum
FITC	Fluorescein isothiocyanate
GAPDH	Glyceraldehyde-3-phosphate dehydrogenase
HLA	Human leukocyte antigen
HRP	Horseradish peroxidase
IFN	Interferon
L929-CM	L929-conditioned medium
M-Mulv RT	Moloney-murine leukemia virus reverse transcriptase
MMPs	Matrix metalloproteinases
MSCs	Mesenchymal stem cells
MTT	3-(4,5-dimethylthiazol-2-yl)-2,5-diphenyltetraxoliumbromide
NAC	N-acetyl-L-cysteine

PARP	Poly (ADP)-ribose polymerase
PBS	Phosphate-buffered saline
PCR	Polymerase chain reaction
PI	Propidium iodide
PS	Penicillin and streptomycin
PTEN	Phosphatase and tensin homolog
PVDF	Polyvinylidene fluoride
RNA	Ribonucleic acid
SCF	Stem cell factor
SD	Standard deviation
TBST	Tris-buffered saline-Tween 20
TIMP	Tissue inhibitor of metalloproteinase
TNF	Tumor necrosis factor
TUNEL	Terminal deoxynucleotidyl transferase-mediated nick-end labeling
UCMS cells	Umbilical cord matrix stem cells
VEGF	Vascular endothelial growth factor
VEGFR	Vascular endothelial growth factor receptor

List of Figures

List of tables

CHAPTER I

Literature review

1. Malignant melanoma and their treatment

Although melanoma accounts for less than 10% of all skin cancers in humans, it is the most deadly because of its propensity for metastatic spread throughout the body (Faião-Flores et al., 2011). The incidence rates of melanoma in the the United States (U.S.) have been continuously increasing over the past 30 years, with the incidence in 2013 estimated at 76,690 new melanoma cases and 9,480 related deaths (Siegel et al., 2013). Globally, melanoma was responsible for approximately 232,000 new diagnoses in 2012, with mortality hot spots in Australia and New Zealand (Ferlay et al., 2014). The overall 5-year survival rate from the diagnosis for patients whose melanomas are detected early, before the tumor has spread to regional lymph nodes or other organs, is about 98% in the U.S., falling to 62% when the disease reaches the lymph nodes, and 15% when the disease metastasizes to distant organs (Balch et al., 2009). In a meta-analysis of patients with metastatic melanoma enrolled in phase II clinical trials, the 1-year survival rate from clinical trial enrollment was approximately 25%, and

median overall survival was only 6 months (Korn et al., 2008). In Korea, the incidence of malignant melanoma increased from 1.02% of all skin malignancies in the 1980s to 15.6% in the 1990s (Lee et al., 2003). In comparison to the cutaneous melanomas arising in Caucasians, they occur more commonly in unusual sites (e.g., hands and feet) in Asians in the form of acral melanoma (Garbe et al., 2000; Lee et al., 2003). Due to the rarity of their occurrences and acral presentations, diagnosis is often delayed, resulting in more advanced stages of disease at presentation (Bae et al., 2009).

Current therapy includes surgery, radiotherapy and chemotherapy. Once the disease becomes metastatic, these treatments are rarely curative and have little benefit, and they do not result in an improvement in overall survival (Lee et al., 2012). Until recently, systemic chemotherapies using dacarbazine, hydroxyurea, or immunotherapy with high-dose interleukin-2 (IL-2) were the only treatment options approved by the U.S. Food and Drug Administration (FDA) for patients with advanced melanoma (Garbe et al., 2011). These agents have not demonstrated improvement in overall survival, nor have they been studied in large randomized phase III trials (Mansfield and Markovic, 2009).

Melanocytic tumors comprise 4-7% of all canine neoplasms and account for 9-20% of skin tumors in dogs (Marino et al., 1995). They are the most common malignant tumors of the oral cavity and of the digits in dogs

(Marino et al., 1995). Dermal melanoma generally is a benign disease that can be cured by local excision; but mucocutaneous melanoma, oral melanoma and uveal melanoma are aggressive tumors that commonly metastasize to the regional lymph nodes and to the lungs,. The malignant melanomas are poorly responsive to the conventional therapy by the time they are discovered (Blackwood and Dobson, 1996; Quintin-Colonna et al., 1996; Todoroff and Brodey, 1979). Wide resection is the most effective modality for eradication of the primary tumor (Schwarz et al., 1991). Given the aggressive biological behavior, adjuvant therapies have been recommended for malignant melanoma, including chemotherapy, radiation therapy, and a xenogeneic DNA vaccine (Boria et al., 2004; Brockley et al., 2013; Proulx et al., 2003). Equivocal data exist regarding the efficacy of chemotherapy (Boria et al., 2004). Recently, Brockley et al. failed to demonstrate improved survival time in dogs with oral melanoma by the use of adjuvant carboplatin following excision (Brockley et al., 2013). The efficacy of the DNA vaccine is similarly equivocal (Grosenbaugh et al., 2011); Ottnod et al failed to show any survival advantage with vaccine use (Ottnod et al., 2013). In order to enhance the efficacy of melanoma therapy, a novel approach is required.

2. Mesenchymal stem cells

Mesenchymal stem cells or multipotent mesenchymal stromal cells (MSCs) are a heterogeneous population of cells that proliferate *in vitro* as plastic-adherent cells, have fibroblast-like morphology, form colonies *in vitro* and can differentiate into bone, cartilage and fat cells. MSCs have been successfully isolated from nearly every organ and many tissues including brain, liver, kidney, lung, bone marrow, muscle, thymus, pancreas, skin, aorta, vena cava, adipose tissue, fetal tissue, umbilical cord, Wharton's jelly and placenta (da Silva Meirelles et al., 2006; Momin et al., 2010; Romanov et al., 2003). MSCs are considered to be promising candidates for clinical application due to the ease of isolation from adult donors, thus obviating the ethical concerns concerning embryonic stem cell research (Yang et al., 2005). MSCs potently modulate immune responses and have paracrine effects through secretion of growth factors, cytokines and antifibrotic or angiogenic mediators (Uccelli et al., 2008). Thus, MSCs have a broad prospect of clinical application in regenerative medicine and cancer therapy. Adipose tissue obtained from subcutaneous tissue represents the most plentiful potential source for harvesting MSCs reliably using a less invasive procedure than that required for other types of MSCs (Zuk et al., 2001). These characteristics make them an attractive source for clinical and research use.

3. The function of MSCs in tumors

MSCs show promising potential for use in regenerative medicine and a variety of diseases because of their self-renewal and multipotential differentiation abilities. In addition to recent studies describing their tissue regeneration capability, MSCs have been identified as promising therapeutic tools in cancer treatment (Khakoo et al., 2006; Pardal et al., 2003; Studeny et al., 2004a; Studeny et al., 2002). MSCs possess a powerful capacity for tumor-directed migration and incorporation, highlighting their potential as optimal vehicles for delivering anticancer agents (Studeny et al., 2004a; Studeny et al., 2002). However, there are several critical questions that need to be addressed in order to develop MSCs as an effective therapy for cancer patients. Many studies have reported contradictory results: some investigators have discovered that MSCs promote tumor growth and others support the hypothesis that MSCs inhibit tumor growth (Klopp et al., 2011; Lazennec and Jorgensen, 2008). The anti-tumor effects of MSCs are highly variable depending on the types of MSCs and tumor cells.

Some studies reporting that MSCs can promote tumor growth are listed in Table 1. Tumors are composed of a heterogeneous mixture of extracellular matrix (ECM), blood vessels, immune and inflammatory cells, connective tissue, and MSCs (Li et al., 2007). It is generally believed that MSCs may be involved in many aspects of regulating immune surveillance, apoptosis, and angiogenesis during tumor development as a source of soluble factors (Hong et al., 2014). Bone marrow-derived MSCs (BM-MSCs) have been

shown to enhance the *in vivo* growth of lymphoma, colon cancer, breast cancer and melanoma cells (Ame-Thomas et al., 2007; Djouad et al., 2003; Karnoub et al., 2007; Zhu et al., 2006). Adipose tissue-derived MSCs (AT-MSCs) exhibit tumor tropism and are thought to be functionally similar to BM-MSCs (Ame-Thomas et al., 2007). Muehlberg et al. (2009) demonstrated that AT-MSCs can promote breast cancer growth in a mouse model (Muehlberg et al., 2009). Human AT-MSCs have also been shown to favor tumor cell growth in nude mice. When human AT-MSCs were co-injected subcutaneously with lung cancer or glioma cells into nude mice, the tumor size was significantly increased compared to the control (Yu et al., 2008).

MSCs have been reported to support the tumor vasculature by differentiating into pericytes and endothelial cells, and secreting vasculogenic growth factors (Al-Khaldi et al., 2003; Roorda et al., 2009). MSCs are generally thought to have immunosuppressive effects, which may be an important mechanism through which MSCs promote tumor growth or increase the incidence of tumor formation (Djouad et al., 2003). Recent *in vitro* studies showed that the immunosuppressive effect of MSCs is mediated through inducible soluble factors such as TNF-α, IL-1α, IL-1β, IFN-γ, IDO, and PGE2 (Yoo et al., 2009).

The inhibition of tumor growth by MSCs has been demonstrated in different types of animal models and the selected studies are listed in Table

2. Using Lewis' lung carcinoma and B16 melanoma experimental models, Maestroni et al. first reported that co-injection of mouse MSCs with tumor cells inhibited primary tumor growth and metastasis (Maestroni et al., 1999). MSCs also exhibited a growth inhibitory effect on mouse tumor cell lines without immunosuppression of the host (Lu et al., 2008). Additional evidence for tumor suppression of MSCs was presented by the inhibition of growth of rat colon carcinoma cells upon subcutaneous co-transplantation in a gelatin matrix (Ohlsson et al., 2003). More recently, the innate anti-tumor effects of MSCs were recognized in the studies on experimental Kaposi's sarcoma, hepatic and pancreatic cancers (Hou et al., 2013; Khakoo et al., 2006; Kidd et al., 2010).

Qiao et al. demonstrated that dermal tissue-derived MSCs from human fetuses were able to inhibit the proliferation of liver cancer cells in a co-culture model, and the inhibitory effects of the MSCs on tumor growth might be associated with downregulation of the Wnt/β-catenin signaling pathway (Qiao et al., 2008b). This study further demonstrated that MSCs inhibit *in vitro* proliferation of breast cancer cells by secreting DKK-1, which in turn suppresses the Wnt/β-catenin signaling pathway (Qiao et al., 2008a). More recently, similar observations have also been reported for hepatocellular carcinoma (Abdel aziz et al., 2011). Their inhibitory effects are associated with downregulation of Wnt-signaling target genes such as β-catenin, PCNA, cyclin D and survivin .

4. Therapeutic potential of MSCs in cancer therapy

One of the newer therapeutic applications of MSCs is a cellular vehicle. Homing directly to the tumor microenvironment, engineered MSCs are able to express and/or release anticancer agents that constantly act on adjacent tumor cells. It has been reported that stromal cell-derived factor-1 (SDF-1)/CXCR4, stem cell factor (SCF)/c-Kit and/or vascular endothelial growth factor (VEGF)/VEGF receptor (VEGFR) 1 and VEGFR 2, may play key roles in tumor-tropic effects (Nakamizo et al., 2005). In addition to the intrinsic anti-tumor properties of MSCs, the presence of MSCs in tumor niches allows any secreted anti-tumor molecules to act locally and efficiently (Dai et al., 2011).

Several studies support the rationale that genetically engineered MSCs can serve as a cellular vehicle to deliver therapeutic agents or cytokines directly into the tumor microenvironment to produce high local concentrations of these therapeutic products at the tumor sites. To date, a number of anticancer agents have been engineered into MSCs and successfully exhibited anticancer effects on various cancer models, including IFN-β on pancreatic, prostate and lung cancers, IFN-α on melanoma, IL-2 on glioma, IL-12 on hepatoma and melanoma, and TRAIL on breast cancer, glioma and lung cancer (Dai et al., 2011; Elzaouk et al., 2006; Kidd et al., 2010; Ren et al., 2008; Seo et al., 2011b; Studeny et al., 2004b). Differing from

conventional therapies, the use of anticancer gene-engineered MSCs enables specific anticancer agents to intensively act on particular targets (Dai et al., 2011).

5. Antitumor role of Interferon-β

The antitumor effects of Interferon-β (IFN-β) are associated with the stimulation of differentiation, S-phase arrest, and apoptosis (Damdinsuren et al., 2003). The cytokine interferon-beta (IFN-β) is known to have potent pro-apoptotic effects and is capable of inhibiting both tumor growth and angiogenesis (Chawla-Sarkar et al., 2001; Jonasch and Haluska, 2001; Kirkwood and Ernstoff, 1984). Considering both anti-proliferative and anti-invasive effects of IFNs, IFN-β has the strongest anti-tumoral effect on human melanoma cells (Horikoshi et al., 1995). IFN-β may mediate anti-tumor effects either indirectly by regulating the immunomodulatory and anti-angiogenic responses or directly by affecting the proliferation or cellular differentiation of tumor cells (Chawla-Sarkar et al., 2003). Despite these activities, clinical trials have failed to identify a clinical benefit for treatment with IFN-β (Einhorn and Grander, 1996). These limited clinical efficacy may result from the short half-life and the systemic toxicities of recombinant IFN-β protein at the doses needed to achieve an antitumor effect (Einhorn and Grander, 1996).

Recent studies indicated that mesenchymal stem cells engineered to secrete IFN-β trafficked to and reduced the tumor burden of melanoma, breast carcinoma, prostate cancer, and lung metastases (Ren et al., 2008; Studeny et al., 2002; Studeny et al., 2004b). Mouse BM-MSCs were transduced by an adenoviral vector (rAAV-IFN-β) carrying the human IFN-β coding sequence and used as cellular vehicles in a prostate cancer model. Following the administration of IFN-β-expressing MSCs, the mice showed reduced prostate tumor volume, increased tumor cell apoptosis, and decreased tumor cell proliferation. The systemic level of IFN-β was not significantly elevated by the administration of IFN-β-expressing MSCs (Ren et al., 2008).

Table 1. Studies reporting that MSCs promote tumor growth

Author	Isolation	Tumor model	MSC:Tumor cell ratio	Results	Proposed mechanism
Djouad et al.	Mouse BM-MSCs	B16 melanoma	1:1 coinjected	Increased incidence	Immunologic
Zhu et al.	Fetal and adult BM-MSCs	Colon cancer cell line (SW480 and F6)	10:1, 1:1 coinjected	Increased incidence	Enhanced proliferation and angiogenesis
Muehlberg et al.	Human and mouse AT-MSCs	Breast (4T1 and MDA231)	10:1 coinjected or i.v. 24 h later	Increased size	Paracrine factor (SDF-1/CXCR secretion)
Karnoub et al. (Karnoub et al., 2007)	Human BM-MSCs	Breast (MCF/Ras, MDA-MB-231, MDA-MB-435 and HMLER)	3:1 coinjected	Increased size in one cell line (MCF/Ras) and increased metastasis	Chemokine secretion (CCL5)
Yu et al.	Human AT-MSCs	Lung cancer (H460) or glioma (U87MG)	1:1, 2:1, 1:10 coinjected	Increased size	Reduced apoptosis
Galie et al.	Mouse AT-MSCs	Breast (BB1)	1:1	Increased incidence and size	Vasculogenic
Lin et al.	Human AT-MSCs	Prostate (PC3)	1:2 injected in contralateral flank after 7 days	Increased incidence and size	Vasculogenic and modulation of tumoral CXCR4
Kucerova et al.	Human AT-MSCs	Mealnoma (A375 and M4Beu) and glioglastoma multiforme (8MGBA)	1:10-1:5 coinjected or i.v. synchronous with tumor injections	Decreased latency and increased size	VEGF and SDF-1α/CXCR4
Prantl et al.	Human AT-MSCs	Prostate	1:10 coinjection subcutaneously	Increased size	Vasculogenic with differentiation into endothelial cells
Shinagawa et al.	Human MSCs	Colon (KM12SM)	1:2 coinjected into cecum	Increased size and metastasis	Increased angiogenesis and reduced apoptosis

Table 2. Studies reporting that MSCs inhibit tumor growth

Author	Isolation	Tumor model	MSC:Tumor cell ratio	Results	Proposed mechanism
Maestroni et al.	BM-MSCs	Lewis lung and melanoma (B16)	1:1 coinjected	Tumor size smaller and decreased metastasis	Increased by treatment of MSC with GM-CSF
Khakoo et al.	Human BM-MSCs	Kaposi sarcoma	3×10^6 MSC injected i.v.	Tumor size smaller	AKT signaling
Qiao et al.	Human fetal skin	Human hepatoma cell line (H7402 and HepG2)	1:1 coinjection	Tumor size smaller	Wnt signaling
Qiao et al.	Human fetal skin	Breast cell line (MCF-7)	1:100 coinjection	Increased latency, reduced tumor size, and metastasis	Wnt signaling
Lu et al.	Mouse BM-MSCs	Hepatoma (H22), lymphoma (Tac-1 and EL-4) and rat insulinoma (INS-1)	2-4:1 i.p. into tumor-bearing mice	Decreased ascites formation	Induced apoptosis and cell cycle arrest in G0/G1 phase
Zhu et al.	Human AT-MSCs	Human myelogenous leukemia (K562) cell line in nude mice	1:10 grown isolation *in vivo*	Proliferation inhibited	Secretion of DKK-1
Otsu et al.	Rat BM-MSCs	Mouse B16F10 melanoma	10^6 into a established 700 mm^3 tumor	Tumor size smaller	Inhibition of angiogenesis
Cousin et al.	Human AT-MSCs	Pancreatic cancer cells	10^3 per mm^3 of established tumor	Tumor size smaller	G1 arrest
Ohlsson et al.	MPC1cE MSCs	Rat colon carcinoma (H1D1)	1:1 and 10:1 in gelatin matrix	Tumor size smaller	Increased inflammatory infiltrate
Dasari et al.	USMS cells	Glioma (SNB19 and U251, 4910 and 5310)	1:4 injected 7 days later into contralateral hemisphere	Decreased tumor size	Upregulation of PTEN
Secchiero et al.	BM-MSCs	Non-Hodgkins lymphoma (SKW6.4 and BJAB)	1:10 and 1:2 injected i.p. 4 days later	Decreased tumor burden with increased survival	Endothelial cell apoptosis *in vitro*

CHAPTER II

Human Adipose Tissue-derived Mesenchymal Stem Cells Inhibit Melanoma Growth *in vitro* and *in vivo*

Abstract

The effects of adipose tissue-derived mesenchymal stem cells (AT-MSCs) on the growth of human malignancies, including melanoma, are controversial and the underlying mechanisms are not yet understood. The aim of this study was to investigate the *in vitro* and *in vivo* anti-tumor effects of human AT-MSCs on human melanoma. The inhibitory effect of AT-MSC-conditioned medium (AT-MSC-CM) on the growth of A375SM and A375P (human melanoma) cells was evaluated using a cell viability assay. Cell cycle arrest and apoptosis in melanoma cells were investigated by flow cytometry and Western blot analysis. To evaluate the *in vivo* anti-tumor effect of AT-MSCs, CM-DiI-labeled AT-MSCs were circumtumorally injected in tumor-bearing athymic mice and tumor size was measured. AT-MSC-CM inhibited melanoma growth by altering cell cycle distribution and inducing apoptosis *in vitro*. AT-MSCs suppressed tumor growth in tumor-bearing athymic mice and fluorescence analysis showed that AT-MSCs

migrated efficiently to tumor tissues. AT-MSCs inhibit the growth of melanoma suggesting promise as a novel therapeutic agent for melanoma.

1. Introduction

Although melanoma accounts for less than 10% of all skin cancers, malignant melanoma is an aggressive disease that accounts for 75% of skin cancer-related deaths (Faião-Flores et al., 2011). The incidence rates of melanoma in the USA have been continuously increasing in the last few decades, with the incidence in 2013 estimated at 76,690 new melanoma cases and 9,480 related deaths (Siegel et al., 2013). Current therapy includes surgery, radiotherapy and chemotherapy. Once the disease becomes metastatic, these treatments are rarely curative and have little benefit, and they do not result in an improvement in overall survival (Lee et al., 2012). For these reasons, several advanced therapeutic strategies have been investigated (Karimkhani et al., 2014; Lee et al., 2012; Olszanski, 2014) as there is definitely an urgent need for novel treatment options with better efficacy.

Mesenchymal stem cells (MSCs) are a fibroblast-like subset of stromal stem cells that can differentiate into bone, cartilage and fat cells. MSCs have been isolated from many adult tissues including: bone marrow, brain, liver, pancreas, skin, adipose tissue, umbilical cord, Wharton's jelly and placenta (da Silva Meirelles et al., 2006; Momin et al., 2010; Orbay et al., 2012; Romanov et al., 2003). Adipose tissue-derived mesenchymal stem cells (AT-MSCs) were first isolated by Zuk *et al*. (Zuk et al., 2001). These adult

stem cells share similar characteristics to bone marrow-derived MSCs (BM-MSCs) with regard to morphology and their ability to undergo differentiation into multiple cell types (Zuk et al., 2001). Adipose tissue can be obtained by less invasive procedures and in larger quantities compared to bone marrow. The yield of MSCs from adipose tissue is about 40-fold higher than the yield from bone marrow (Kern et al., 2006). These features make adipose tissue an attractive candidate for clinical and therapeutic use.

MSCs have the ability for self-renewal and differentiation into multiple cell types and they, therefore, hold great promise for tissue repair and regenerative medicine. In recent years, MSCs have been receiving increased attention because they were shown to be capable of migrating towards tumor sites. This property has led to the use of MSCs as vehicles to deliver therapeutic agents, such as cytokines, apoptosis inducers, pro-drugs and interferons to tumor sites for growth inhibition (Belmar-Lopez et al., 2013; Chen et al., 2012; Studeny et al., 2002; TANG et al., 2014; Wang et al., 2014). Further, MSCs genetically engineered to produce antitumor molecules have shown strong therapeutic effects in experimental melanoma models (Chen et al., 2012; Elzaouk et al., 2006; Studeny et al., 2002). However, very few studies have investigated the antitumor properties of MSCs themselves and their impact on tumor progression is still under debate. Some studies have suggested that MSCs inhibit tumor growth (Hou et al., 2014; Qiao et al., 2008a), while others believe that MSCs promote

tumor progression and metastasis (Xu et al., 2009; Yan et al., 2012). For example, Sun et al. reported that BM-MSCs promoted proliferation of tumor cells and improved the microenvironment in B16 mouse melanoma cells (Sun et al., 2008). Thus, the antitumor effect of MSCs on the targeted tumor should be further investigated prior to their use as delivery vehicles for tumor-targeted gene therapy.

This study investigated the *in vitro* and *in vivo* anti-tumor potential of AT-MSCs in melanomas. It was found that AT-MSC-conditioned medium (AT-MSC-CM) suppresses melanoma proliferation and can significantly induce cell cycle arrest and apoptosis in the melanoma cell lines A375SM and A375P. It was also observed that treatment with AT-MSCs reduced the tumor volume in melanoma-bearing athymic nude mice. These findings suggest that AT-MSCs have favorable anticancer characteristics and should be further explored in future studies on melanoma therapy.

2. Materials and methods

2.1. AT-MSC isolation and culture

Human adipose tissue samples were obtained by liposuction from abdominal subcutaneous fat after informed consent of the donors was obtained. AT-MSCs were prepared in accordance with the Good Manufacturing Practice guidelines (K-STEMCELL CO. Ltd., Seoul, Korea) as described previously (Choi et al., 2011). Briefly, subcutaneous adipose tissues were digested with collagenase I (1 mg/ml) under gentle agitation for 60 min at 37℃. The digested tissues were filtered through a 100-μm nylon sieve to remove cellular debris and were collected by centrifugation at 470 x *g* for 5 min. The cell pellet was re-suspended in RCME (K-STEMCELL media for MSC attachment, K-STEMCELL) containing 10% fetal bovine serum (FBS). The cell suspension was re-centrifuged at 470 x *g* for 5 min. The supernatant was discarded and the pellet was collected. The cell fraction was cultured overnight at 37℃ in 5% CO_2 in RCME containing 10% FBS. Non-adherent cells were removed after 24 h and the medium was changed to RKCM (K-STEMCELL media for MSC growth, K-STEMCELL) containing 5% FBS. The cells were maintained for 4–5 days until they reached confluence (passage 0). When the cells reached 90% confluence, they were expanded in RKCM until passage 3. Cell viability as evaluated by

trypan blue exclusion before transplantation was greater than 95%. No evidence of bacterial, fungal or mycoplasma contamination was observed. Cell surface markers expressed by the AT-MSCs were analyzed using a FACS Calibur flow cytometer (BD Biosciences, San Jose, CA) with the CELL Quest software (Becton Dickinson, San Jose, CA). The AT-MSCs were positive for CD29, CD44, CD73, CD90, CD105 and HLA-ABC but were negative for CD31, CD34, CD45 and HLA-DR. AT-MSCs were used at passages 3–6 and subcultured once before use.

2.2. Cancer cell culture

A375SM, A375P (both human melanoma cell lines) and L929 (murine fibroblast cell line) cells were purchased from the Korea Cell Line Bank (Seoul, Korea). Melanoma cells were cultured in high-glucose Dulbecco's modified Eagle medium (DMEM; Hyclone, Logan, UT, USA) containing 10% heat-inactivated FBS (Hyclone, Logan, UT), 1% penicillin and streptomycin (PS, Hyclone), 1.5 g/l sodium bicarbonate (Sigma-Aldrich, Strinheim, Germany) and 10 mM 4-(-2-hydroxyethyl)-1-piperazine ethanesulphonic acid (Hyclone). L929 cells were cultured in high-glucose DMEM containing 10% heat-inactivated FBS and 1% PS. Media supplementation or replenishment was carried out every 2–3 days.

2.3. Preparation of conditioned media

Conditioned media derived from L929 cells and AT-MSCs were prepared as follows: 1×10^6 of each of the cells was cultured on 10-cm plates with 10 ml of a 1:1 mixture of DMEM and Ham's F12 (DME/F12, Hyclone), 5% FBS and 1% PS for 48 h. The medium was harvested and filter-sterilized using a 0.22-μm Millex-HV syringe filter (Millipore, Billerica, MA, USA) and stored at -80℃ until use.

2.4. *In vitro* cell viability assay

The percentage of viable A375SM and A375P cells was evaluated using the MTT (3-(4,5-dimethylthiazol-2-yl)-2,5-diphenyltetraxoliumbromide) assay. The human melanoma cells (2×10^4/well) were cultured in complete medium in 24-well plates for 24 h. The cells were cultured in triplicate with or without AT-MSC-CM and L929-conditioned medium (L929-CM) for another 72 h; the medium was replaced with fresh medium every 24 h. Control cells were cultured in DME/F12 1:1 medium supplemented with 5% FBS. Cell viability was measured by the MTT assay according to the manufacturer's recommendations (Sigma, St. Louis, MO, USA). Briefly, 10 μl of MTT reagent (final concentration, 0.5 mg/ml) was added to the culture dishes and incubated for 2 h until a purple precipitate was visible. The

supernatant was then aspirated and 100 µl of the detergent reagent was added. Absorbance at 540 nm was spectrophotometrically measured using a microplate ELISA reader (Bio-Rad, Hercules, CA, USA) with a reference wavelength of 630 nm. The results are expressed as the percentage of the values obtained in control conditions.

2.5. Cell cycle analysis

For flow cytometry (FACS) analysis, A375SM and A375P cells (1×10^5 cells) were plated in 60-mm culture plates and cultured with AT-MSC-CM as described in the "*in vitro* cell viability assay" section. After 3 days, the cells were trypsinized, counted and fixed with 70% ethanol. For analysis of DNA content, the cells were labeled with propidium iodide (PI) (Sigma-Aldrich) in the presence of RNaseA (Sigma-Aldrich) (50 µg/ml, 30 min, 37°C in the dark). Samples were run on a FACScan flow cytometer (Becton-Dickinson, FL, NJ, USA) and data were analyzed using FCS Express 4 (De Novo Software, Thornhill, Ontario, Canada).

2.6. Annexin V-FITC assay

A375SM and A375P cells (1×10^5 cells) were plated in 60-mm culture plates and cultured with AT-MSC-CM for 72 h. The cells were then

disassociated using trypsin-EDTA (Invitrogen) and washed with Annexin V binding buffer (1X). The cells were then labeled with either annexin-FITC (BioVision, Mountain View, CA, USA) or PI as per the manufacturer's recommendations. Briefly, melanoma cells were collected by centrifugation and re-suspended in 500 µl of binding buffer. Then, 5 µl of Annexin V-FITC was added to the re-suspended cells. After incubation for 5 min on ice in the dark, 1 µg of PI was added to the cell suspension. Apoptotic and necrotic cells were quantified using a FACScan flow cytometer and the Cell Quest pro software (Beckton-Dickinson).

2.7. Western blot analysis

For western blot analysis, A375SM and A375P cells were cultured with AT-MSC-CM for 72 h. Proteins were extracted from A375SM and A375P cells, resolved on SDS-polyacrylamide gels and transferred to a polyvinylidene fluoride (PVDF) membrane (Whatman, Maidstone, UK). The transferred membranes were blocked with 5% skim milk in Tris-buffered saline-Tween 20 (TBST: 0.1% Tween 20, 100 mM NaCl and 10 mM Tris-HCl, (pH 7.6)) for 2 h at room temperature. Blots were incubated with antibodies against cyclin D1, procaspase-3 and caspase-7 (1:250, 1:500 and 1:500 dilution, respectively) purchased from Santa Cruz Biotechnology Inc. (Heidelberg, Germany). Poly (ADP)-ribose polymerase (PARP) and β-

actin antibodies (1:1000 and 1:5000 dilution, respectively) were purchased from Cell Signaling Technology (Ozyme, St Quentin en Yvelines, France). Secondary horse radish peroxidase (HRP)-conjugated antibodies (1:2000 dilution; Santa Cruz, Heidelberg, Germany) were added and blots were incubated in a blocking buffer for 2 h at room temperature. Immunoreactive proteins were visualized using the ECL plus kit (Gendepot, TX, USA).

2.8. Scratch wound-induced migration assay

Wound-induced migration assay was performed to assess the effect of AT-MSC-CM on melanoma cell migration as previously described (Vaid et al., 2011). Briefly, melanoma cells were grown till they reached full confluence in 24-well plates coated with 2% gelatin and incubated overnight in starvation medium. Cell monolayers were wounded with a sterile 1-ml pipette tip and washed with phosphate-buffered saline (PBS) to remove the detached cells from the plates. Cells were either left untreated or treated with conditioned medium and kept in a CO_2 incubator for 64 h. The medium was replaced with fresh medium every 24 h. The wound gap was observed and cells were photographed using phase-contrast microscopy. The images were then analyzed using the Image J software 1.45s version (National Institutes of Health, USA) to measure the width of the scratch. The relative migration distance was calculated using the following formula: relative

migration distance (%) = 100 (*a*-*b*)/*a*, where *a* represents the width of the cell wounds before incubation and *b* represents the width of the cell wounds after incubation.

2.9. Nude mouse transplantation

Female, 6-week-old BALB/c nude mice were purchased from Central Lab. Animal, Inc. (Seoul, Republic of Korea). The mice were housed in a specific pathogen-free facility and allowed to acclimatize for 1 week to ensure that they were healthy before the start of the *in vivo* study. All animals were handled in strict accordance with the recommendations of the Guide for the Care and Use of Laboratory Animals of the National Institutes of Health. The protocol was approved by the Seoul National University Institutional Animal Care and Use Committee. To induce human melanoma development in the mice, A375SM cells (5.0×10^6), suspended in 200 μl PBS, were injected subcutaneously (*s.c.*) into the flanks of the mice. After 2 weeks, the mice that had developed tumors were randomly divided into two groups (n = 5 for each group). Mice in the control group were administered a circumtumoral injection of PBS (100 μl). The mice in the AT-MSC group were treated with AT-MSCs (5.0×10^5 cells) labeled with CM-DiI in PBS (100 μl); they were not given an intratumoral injection but an injection around the tumor site. PBS/AT-MSCs were injected five times every 3 days

(on days 0, 3, 6, 9 and 12). Tumor size was measured every 3 days with a vernier caliper (Mitutoyo, Tokyo, Japan). Tumor volume was calculated using the following formula: tumor volume (mm^3) = ($a^2 \times b$)/2, where *a* and *b* represent the short and long axes respectively.

2.10. Fluorescence staining analysis

Fluorescence staining was performed to detect the presence of AT-MSCs at the tumor locus. Three days after the last injection of CM-DiI-labeled AT-MSCs, mice were sacrificed and tumor tissues were harvested. Tumor tissues were fixed in cold 4% paraformaldehyde for 4 h and then transferred to a sucrose medium (30% sucrose in 0.1 M PBS) for 16 h at 4℃. The tissues were then embedded in Tissue Tek OTC compound (Sakura Finetek, Torrance, CA, USA), snap-frozen in liquid nitrogen and stored at -80℃. The frozen tissue was sectioned (15-μm-thick sections) and mounted on slides. The nuclei of all the cells were stained with Hoechst 33342 (10 μg/ml) for 30 min in the dark. Images were captured with a confocal microscope (Nikon, Eclipse TE200, Tokyo, Japan) and processed using the Image J software 1.45s version.

2.11. Statistical analysis

All experimental data were analyzed using the GraphPad Prism (version 4) software (Graphpad Software Inc., San Diego, CA, USA). All data are presented as mean ± standard deviation (SD). The statistical significance of mean values in multiple sample groups was examined using Bonferroni's comparison test after one-way ANOVA. Statistical differences between the mean values of the two sample groups were determined using the Student's *t* test. *P*-values <0.05 were considered to indicate statistical significance.

3. Results

3.1. *In vitro* inhibition of melanoma cell growth by AT-MSC-CM

AT-MSC-CM significantly inhibited the viability of A375SM (75.09% *vs*. control cells, $p < 0.001$) and A375P (75.41% *vs*. control cells, $p < 0.001$) cells (Figure 1). Because the observed responses may reflect the exhaustion of nutrients from media or the non-specific accumulation of toxic metabolites, conditioned medium from L929 fibroblast cells was used as a control, together with non-conditioned medium. In contrast to AT-MSC-CM, treatment with L929-CM did not impair melanoma cell viability. These results show that AT-MSC-CM has *in vitro* anti-proliferative effects against human melanoma cells.

3.2. Effect of AT-MSC-CM on the cell cycle of melanoma cells

The cell cycle status of A375SM and A375P cells was analyzed 72 h after the cells were cultured with AT-MSC-CM (Figure 2). The amount of melanoma cells cultured with AT-MSC-CM showed an increase in the G0/G1 phase of the cell cycle compared to the controls, which suggests that more melanoma cells are arrested at the G0/G1 phase in the presence of AT-MSC-CM. The proportion of cells in the G0/G1 phase was 65.20% and

50.73% for A375SM cells treated with and without AT-MSC-CM respectively ($p < 0.001$, Figure 2A and 2B); further, it was 72.63% and 61.18% for A375P cells treated with and without AT-MSC-CM respectively ($p < 0.0001$, Figure 2C and 2D). This increase was coupled with a decreased percentage of tumor cells in the S phase. The percentages of A375SM and A375P cells cultured with AT-MSC-CM in the S phase was 19.08% and 18.89%, respectively, whereas it was 32.44% and 28.99%, respectively, for A375SM and A375P cells cultured in control medium ($p < 0.0001$ and $p < 0.0001$ for A375SM and A375P cells, respectively). Next, the expression of the main proteins involved in cell cycle regulation was measured. The expression of cyclin D1 in melanoma cells cultured with AT-MSC-CM for 72 h was decreased (Figure 2E). These results indicate that AT-MSC-CM induces G0/G1 cell cycle arrest of melanoma cells by down-regulation of cyclin D1 expression.

3.3. Apoptotic effect of AT-MSC-CM on melanoma cells

A375SM (Figure 3A) and A375P (Figure 3B) cells were analyzed by flow cytometry with Annexin V/PI staining after culture with AT-MSC-CM for 72 h. As shown in Figure 3C, the apoptosis rates were 5.66% and 5.52% for A375SM and A375P cells, respectively; for the control A375SM and A375P cells, the apoptosis rates were 3.85% and 4.52%, respectively. The apoptosis

rates of cells treated with AT-MSC-CM were significantly different from those of the control cells ($p < 0.01$ for both A375AM and A375P cells). The effects of AT-MSC-CM on procaspase-3, caspase-7 and PARP levels were analyzed by Western blotting to elucidate the underlying biochemical mechanisms involved in the regulation of apoptosis. The procaspase-3 expression in melanoma cells cultured with AT-MSC-CM was down-regulated, whereas cleaved PARP and caspase-7 expression showed a marked increase. These findings show that AT-MSC-CM can induce melanoma cell apoptosis through caspase-3/7 and PARP activation.

3.4. Effect of AT-MSC-CM on human melanoma cell migration

The wound-induced migration assay showed that the major part of the gap or wounding space between cell layers after wounding was occupied by the migrating melanoma cells that were treated with the control medium and L929-CM (Figure 4A and 4B). However, the healing of the wound or the empty space in the cells was largely not occupied by migrating cells treated with AT-MSC-CM. As shown in Figure 4C, relative to L929-CM-treated and untreated control cells, AT-MSC-CM-treated A375SM, as well as A375P cells, showed reduced migration capacity. These findings suggest that AT-MSC-CM inhibited the migration of melanoma cells.

3.5. Melanoma suppression by AT-MSCs in the mouse xenograft model

To evaluate AT-MSC-dependent growth inhibition of human melanoma, a xenograft study of A375SM cells was carried out using female athymic mice. Fourteen days after tumor engraftment, mice were given circumtumoral AT-MSCs or PBS (control). The control tumors grew rapidly and their average size was 2,907.5 ± 843.5 mm^3 within 27 days following transplantation of AT-MSCs (Figure 5A and 5B). In contrast, the tumor volumes were significantly reduced in the AT-MSC group (1,496.8 ± 434.4 mm^3, $p < 0.05$). To confirm the migration of transplanted AT-MSCs to melanoma cells in the A375SM cell xenograft model, AT-MSCs were labeled with the cell tracker dye CM-DiI before *in vivo* administration. Three days after the last administration of AT-MSCs in mice, the tissue was harvested and frozen tumor sections were made. The Hoechst 33342-stained cell nuclei appeared blue and the CM-DiI-labeled AT-MSCs were red in the confocal fluorescence micrograph (Figure 6). These results suggest that circumtumorally injected AT-MSCs effectively migrate to the tumor region.

4. Discussion

Cancer remains one of the major causes of mortality and morbidity throughout the world. The common conventional approaches of surgery, chemotherapy and radiotherapy are often limited by the recurrence of metastasis or therapy-related life-threatening complications (Dai et al., 2011). Despite the development of various tumor-targeted therapeutic methods, the overall outcome of cancer patients has not remarkably improved. For these reasons, there is an urgent need for alternative therapeutic strategies that specifically target malignant cells.

MSCs are a population of adult stem cells with the potential for self-renewal and differentiation into multiple cell types. There is ample evidence that AT-MSCs and other MSC types abolish tumor growth *in vitro* and *in vivo*. For example, human BM-MSCs have been shown to inhibit tumor growth in immunodeficient mice bearing disseminated non-Hodgkin's lymphoma xenografts (Secchiero et al., 2010). Further, another study has demonstrated that rat umbilical cord matrix stem (rUCMS) cells completely attenuated rat mammary adenocarcinoma with no evidence of metastasis or recurrence after the tumor was inoculated with rUCMS cells (Ganta et al., 2009). Anti-tumor effects were also demonstrated in MSCs harvested from adipose tissues. Cousin et al. showed that a single intra-tumoral injection of AT-MSCs in a model of pancreatic adenocarcinoma inhibited tumor growth (Cousin et al., 2009). More recently, AT-MSC-CM was shown to

significantly inhibit the growth of human U251 glioma cells *in vitro* (Yang et al., 2014). Yang et al. also found that the growth of several other tumor cell lines, including the rectal cancer cell line HT29, lung cancer cell line A549 and breast cancer cell line MCF-7, was inhibited by AT-MSC-CM (Yang et al., 2014). However, there are several critical questions to be addressed in order to develop effective treatments for cancer therapy. In contrast to the findings mentioned above, some studies showed that MSCs resulted in systemic immunosuppression that favored tumor growth *in vivo* (Han et al., 2011). For example, Sun et al. found that BM-MSCs played an important role in tumor angiogenesis and promoted proliferation of melanoma cells (Sun et al., 2008). Although MSCs have received attention for their potential use in clinical therapy, there are still several unsolved problems that limit the application of MSCs .

This study aimed to evaluate the effect of AT-MSCs on melanoma growth in two experimental systems and the mechanisms by which AT-MSCs exert their actions. First, the effect of AT-MSCs on tumor cell proliferation was investigated by treatment of tumor cells with AT-MSC-CM. These results clearly showed that AT-MSC-CM can inhibit the proliferation of A375SM and A375P melanoma cells *in vitro*. Khakoo et al. reported that MSCs inhibit the growth of Kaposi's sarcoma by cell-to-cell contact (Khakoo et al., 2006). However, the present study found that the proliferation of melanoma cells was inhibited after melanoma cells were

treated with AT-MSC-CM, which indicates that certain soluble factors secreted by AT-MSCs may inhibit melanoma cell proliferation without cell-to-cell contact. In support of this, it has been reported that the regulatory elements in cell-conditioned medium may influence various signaling mechanisms, such as transcription initiation, differential gene expression and re-programming of specific cell types (Yang et al., 2014). However, the putative molecules in the conditioned medium responsible for altering the cell fate still remain unclear and require further research.

Tumorigenesis is the result of cell cycle disturbance, which leads to uncontrolled cellular proliferation. Cell proliferation and differentiation are specifically controlled in the G1 phase and the G1/S phase transition in the cell cycle (Golias et al., 2004). In our study, a higher amount of A375SM and A375P cells treated with AT-MSC-CM were found in the G0/G1 phase compared to the controls. Therefore, there is reason to believe that AT-MSC-CM represses cell growth *via* cell cycle arrest in the G0/G1 phase. In this report, cyclin D1 levels decreased in A375SM and A375P cells treated with AT-MSC-CM, which probably indicates that AT-MSC-CM can down-regulate the cyclin D1 protein level, ultimately leading to cell cycle arrest of melanoma cells. The main families of regulatory proteins that play major roles in controlling cell-cycle progression are the cyclin-dependent kinases (Cdks), cyclins, the Cdk inhibitors (CKI) and the tumor-suppressor gene products p53 and pRb (Gali-Muhtasib and Bakkar, 2002). It is, therefore,

possible that AT-MSC-CM disrupts these cell cycle regulatory mechanisms in A375SM and A375P cells.

To determine the mechanism by which AT-MSC-CM inhibited melanoma cell proliferation, Annexin V/PI flow cytometric assays were performed. The flow cytometric assay indicated that AT-MSC-CM can induce apoptosis in A375SM and A375P cell lines. Caspases play a key role in various forms of apoptosis (Cohen, 1997). It is widely believed that activation of caspase-3/7 leads to DNA fragmentation, a hallmark of apoptosis. In the present report, the procaspase-3 levels decreased and caspase-7 levels increased in A375SM and A375P cells treated with AT-MSC-CM. It was, therefore, assumed that up-regulation of cleaved caspase-3 leads to down-regulation of procaspase-3. PARP is from a family of proteins involved in a number of cellular processes that play a role in DNA repair, DNA stability and programmed cell death (Dasari et al., 2010b). It has been reported that caspase-3 and caspase-7 are the most efficient proteases for PARP cleavage (Herceg and Wang, 2001). In the present study, cleaved PARP was up-regulated in A375SM and A375P cells treated with AT-MSC-CM. These findings indicate that AT-MSC-CM can trigger caspase-3/7 activation and, thus, PARP cleavage in melanoma cells ultimately leading to apoptosis. These results are also consistent with the findings of Takahara et al., according to which AT-MSCs induced apoptosis of prostate cancer cells by activating the caspase 3/7 signaling pathway

(Takahara et al., 2014). They have shown that the anti-proliferative effect of AT-MSCs on prostate cancer cells appears to be mediated by TGF-β1 secretion and signaling.

In this study, AT-MSC-CM was found to inhibit the movement of A375SM and A375P melanoma cells. These observations suggest that AT-MSCs secrete a chemical mediator that inhibits the migratory capacity of melanoma cells. Although the exact mechanism could not be determined, these findings are in agreement with recent reports showing that MSCs inhibit the migration and invasion of cancer cells (Clarke et al., 2014; Dasari et al., 2010a; Li et al., 2010). TIMP-1, TIMP-2 and inhibitors of matrix metalloproteinases (MMPs) were identified as candidates for this inhibition (Clarke et al., 2014). Another study has demonstrated that the inhibitory effect on tumor migration was mediated by up-regulation of phosphatase and tensin homolog (PTEN) in glioma cells by cord blood MSCs (Dasari et al., 2010a).

To evaluate the therapeutic effects of AT-MSCs *in vivo*, a melanoma xenograft model was created by injecting human melanoma A375SM cells into the flanks of mice. When AT-MSCs were administered circumtumorally in tumor-bearing nude mice, tumor growth was inhibited. The homing of MSCs to tumors is well-established (Nakamizo et al., 2005). In this study too, AT-MSCs were administered circumtumorally and could find their way into tumors. This homing ability of MSCs seems to be mediated by

chemokines and growth factors secreted by the tumors or their associated stroma (Belmar-Lopez et al., 2013; Dai et al., 2011). The homing ability of MSCs has previously been exploited for drug delivery and targeted gene delivery (Moniri et al., 2012; Seo et al., 2011b; TANG et al., 2014; Wang et al., 2014). The ability of unengineered AT-MSCs to inhibit melanomas is a distinct advantage because any manipulation causing the cells to express an exogenous gene could alter them in some way that would potentially make them less safe as transplantable cells.

In conclusion, this study have provided evidence to suggest that AT-MSC-CM has an anti-proliferative effect on melanoma cells, which is brought about *via* cell cycle arrest and apoptosis of tumor cells, and that AT-MSCs have an inhibitory effect on the growth of A375SM cell-derived tumors *in vivo*. Since AT-MSCs are easily obtained without any ethical concerns, cell therapy using AT-MSCs appears to have promise as a therapeutic option for melanoma, although further research on the clinical application of AT-MSCs is needed.

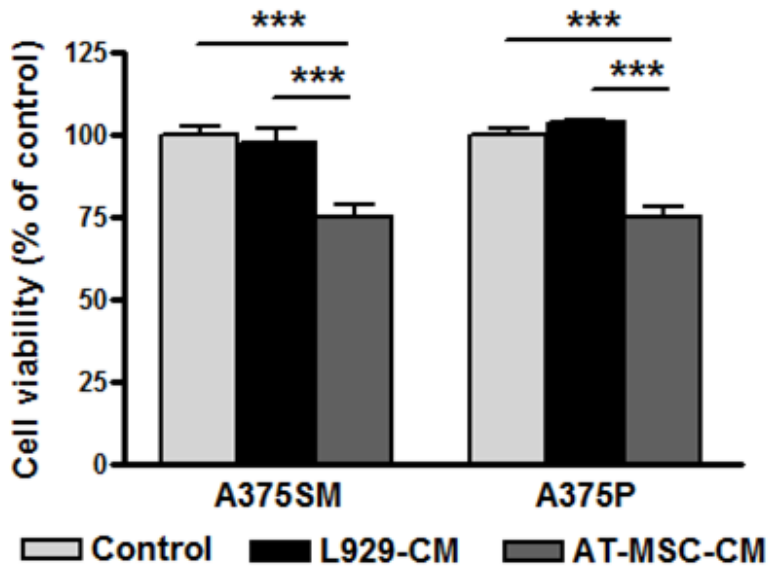

Figure 1. Inhibitory effect of AT-MSC-CM on melanoma cell growth and viability.

Human melanoma cells (A375SM and A375P) were cultured with AT-MSC-CM or L929-CM for 72 h. AT-MSC-CM significantly inhibited the growth of A375SM and A375P cells. Cell viability was ascertained by MTT cell proliferation assay. The results are expressed as percentage of values obtained in control conditions. All experiments were independently conducted in triplicate and values expressed as the mean ± SD. The *p*-value was obtained using one-way ANOVA with *post-hoc* Bonferroni's multiple comparison (*** $p < 0.001$).

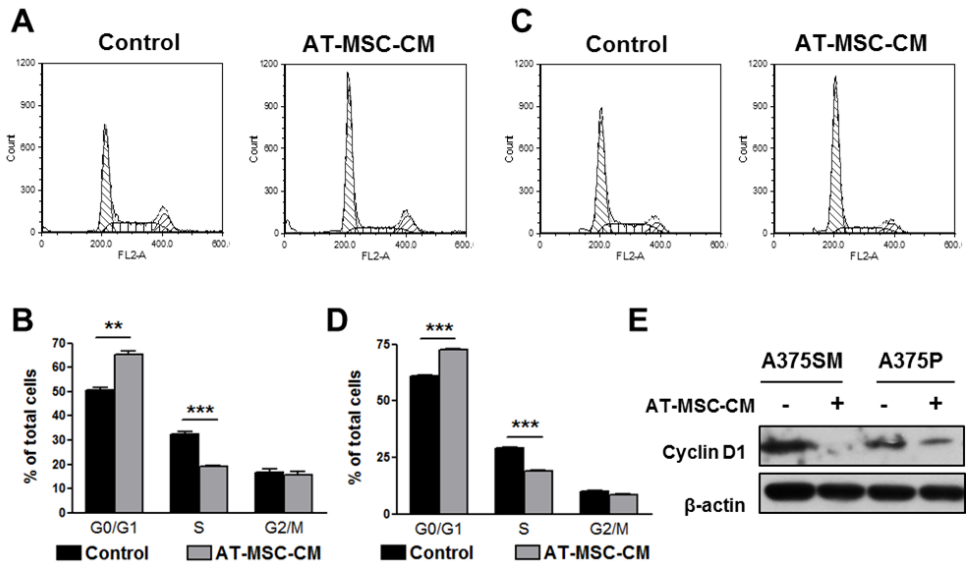

Figure 2. Cell cycle arrest of A375SM and A375P treated with AT-MSC-CM.

The cell cycle phase distribution of (A, B) A375SM and (C, D) A375P was analyzed after harvest by flow cytometery. The melanoma cells treated with AT-MSC-CM showed an increase in the G0/$G1_1$phase of the cell cycle compared to the controls ($p < 0.001$ and $p < 0.0001$, A375SM and A375P, respectively). G1 arrest occurred concurrently with a reduction in the percentage of S phase cells ($p < 0.0001$). All experiments were independently conducted in triplicate and values expressed as the mean ± SD. The *p*-value was obtained using theStudent's t test by comparing treated AT-MSC-CM with control for each phase of the cell cycle (** $p < 0.001$, *** $p < 0.0001$). (E) The expression of cyclin D1 in tumor cells was

detected by Western blotting. Data are representative of three independent experiments.

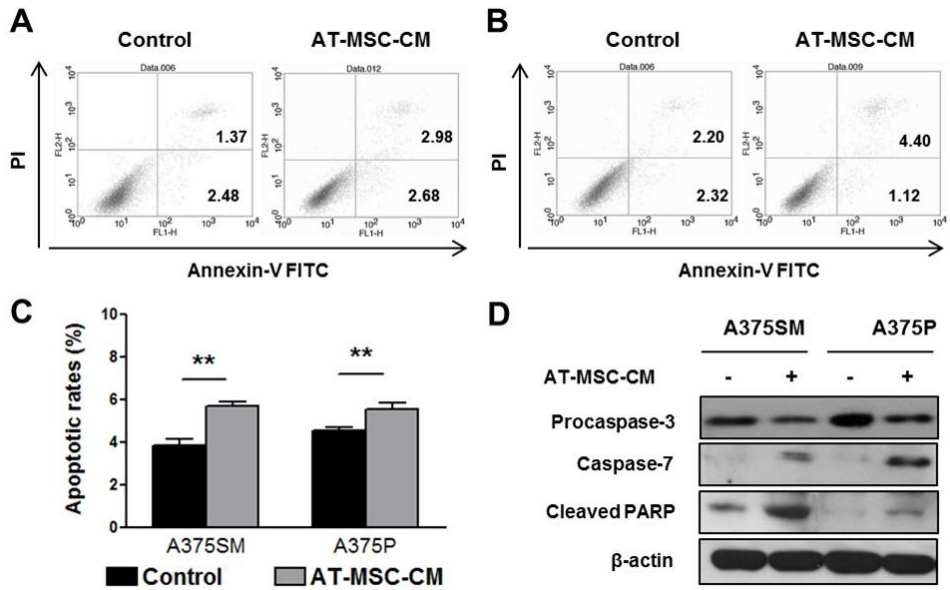

Figure 3. The apoptotic effect of AT-MSC-CM on A375SM and A375P cells.

A375SM and A375P cells were treated with AT-MSC-CM for 72 h. Apoptotic cells of (A) A375SM and (B) A375P were measured by FACS analysis after Annexin V and PI staining. (C) The apoptosis rates of the AT-MSC-CM groups were significantly different from that of the control groups ($p < 0.01$ for both A375SM and A375P cells). All experiments were independently conducted in triplicate and values expressed as the mean ± SD. The *p*-value was obtained using the Student's t test (** $p < 0.01$). (D) The expression of procaspase-3, caspase-7 and cleaved PARP and in tumor cells was detected by Western blotting. Samples were standardized according to β-actin protein levels.

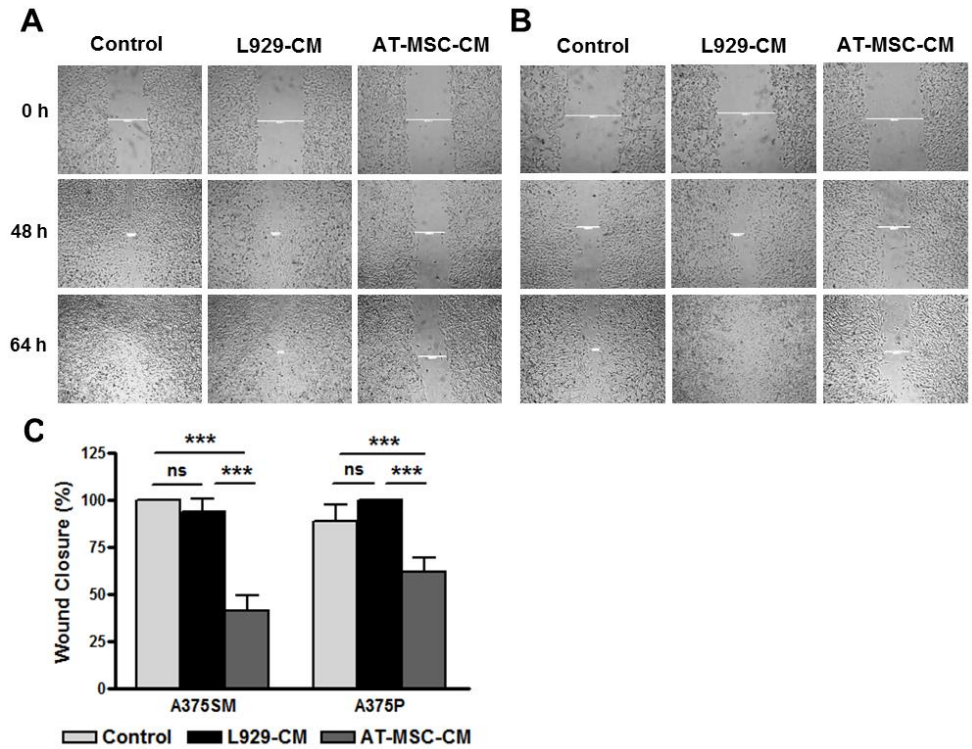

Figure 4. Effects of AT-MSC-CM on migration of A375SM and A375P cells *in vitro*.

Wound-induced migration assay was performed to assess the effect of AT-MSC-CM on the migration of (A) A375SM and (B) A375P cells. The results demonstrated that cell migration into the wound area was significantly inhibited in AT-MSC-CM-treated melanoma cells compared to control and L929-CM-treated cells. The assay was repeated three times and representative pictures are shown. (C) Quantitative analysis of wound-induced migration assay from (A) and (B). All experiments were independently conducted in triplicate and values expressed as the mean ±

SD. The *p*-value was obtained using one-way ANOVA with *post-hoc* Bonferroni's multiple comparison (*** $p < 0.001$).

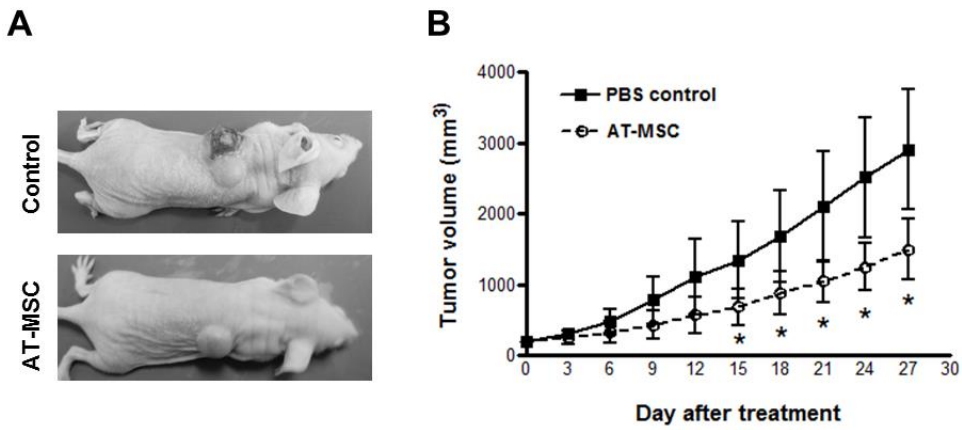

Figure 5. The effect of AT-MSCs on A375SM melanoma growth in BALB/C nude mice.

A total of 5.0×10^6 A375SM cells were inoculated subcutaneously into the flank of each mouse and AT-MSCs were injected circumtumorally in the treatment group. The size of each tumor mass was measured every 3 days with Vernier caliper. (A) Representative tumors on day 15 in athymic nude mice. (B) Tumor volumes were significantly reduced in AT-MSC treatment group in comparison with mice that received PBS as a control. Values were expressed as means ± SD and determination of statistical significance was performed using a Student's t test (* $p < 0.05$).

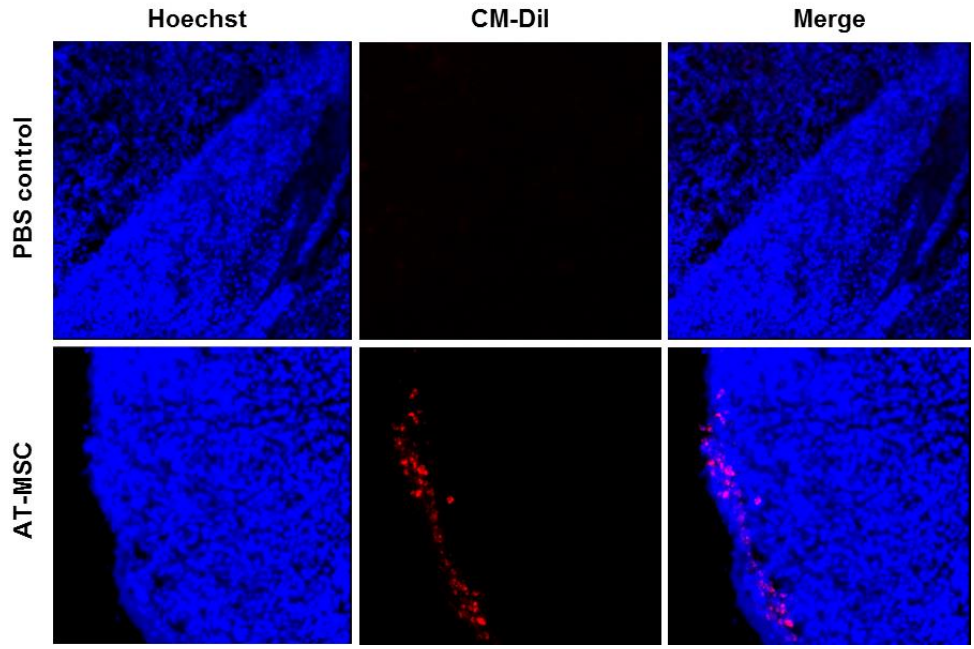

Figure 6. Fluorescence images of AT-MSCs in melanoma tumor tissue.

AT-MSCs were labeled with CM-DiI and injected into tumor-bearing nude mice. Circumtumorally administered CM-DiI labeled AT-MSCs integrated into tumor locus. Sections were counterstained with Hoechst 33342 nuclear stain (blue). CM-DiI labeled AT-MSCs (red) and A375SM melanoma tumor cells identified by confocal fluorescence microscopy of tumor sections. Magnification x 200.

CHAPTER III

Anti-tumor effect of adipose tissue-derived mesenchymal stem cells expressing interferon-β and treatment with cisplatin in a xenograft mouse model for canine melanoma

Abstract

Adipose tissue-derived mesenchymal stem cells (AT-MSCs) are attractive cell-therapy vehicles for the delivery of anti-tumor molecules into the tumor microenvironment. The innate tropism of AT-MSCs for tumors has important implications for effective cellular delivery of anti-tumor molecules, including cytokines, interferon, and pro-drugs. The present study was designed to determine the possibility that the combination of stem cell-based gene therapy with low-dose cisplatin would improve therapeutic efficacy against canine melanoma. The IFN-β transduced canine AT-MSCs (cAT-MSC-IFN-β) inhibited the growth of LMeC canine melanoma cells in direct and indirect *in vitro* co-culture systems. In animal experiments using BALB/c nude mouse xenografts, which developed by injecting LMeC cells,

the combination treatment of cAT-MSC-IFN-β and low-dose cisplatin significantly reduced tumor volume compared with the other treatment groups. Fluorescent microscopic analysis with a TUNEL (terminal deoxynucleotidyl transferase-mediated nick-end labeling) assay of tumor section provided evidence for homing of cAT-MSC-IFN-β to the tumor site and revealed that the combination treatment of cAT-MSC-IFN-β with low-dose cisplatin induced high levels of cell apoptosis. These findings may prove useful in further explorations of the application of these combined approaches to the treatment of malignant melanoma and other tumors.

1. Introduction

Malignant melanoma represents a significant and growing public health threat worldwide. The incidence of melanoma is rising (Wingo et al., 1999) and deaths from malignant melanoma are increasing (Greenlee et al., 2000). Surgical attempts at complete excision rarely are successful, and local recurrence is common (Freeman et al., 2003; Rassnick et al., 2001). Once the disease becomes metastatic, standard chemotherapy has little effect (Armstrong et al., 1996). As in humans, canine malignant melanoma is an aggressive and invasive neoplasm (Freeman et al., 2003). Complications from distant metastatic lesions such as those found in the lung, liver, and regional lymph nodes commonly occur (Freeman et al., 2003; Modiano et al., 1999). For these reasons, several alternative therapeutic strategies have been investigated (Nakaya et al., 2001; Parmiani and Colombo, 1995; Rigel and Carucci, 2000). In order to enhance the efficacy of melanoma therapy, a novel approach is required.

Mesenchymal stem cells (MSCs) are considered to be a promising platform for cell and gene therapy for a variety of diseases (Ozawa et al., 2008). MSCs can routinely be isolated from several organs such as fetal liver, umbilical cord blood, bone marrow, and adipose tissue (Kern et al., 2006; Schaffler and Buchler, 2007; Wagner et al., 2005). They have an extensive proliferative potential and the capacity to differentiate into various

cell types. Compared to the other MSCs, adipose tissue-derived mesenchymal stem cells (AT-MSCs) are easier and simpler to isolate. AT-MSCs can be obtained in large quantities with a less invasive and less painful clinical procedure than that required for other types of MSCs. Importantly, the innate tropism of MSC for tumors makes these cells particularly effective for the cellular delivery of anti-cancer molecules including cytokines, interferons, or pro-drugs (Kidd et al., 2010; Kim et al., 2006; Studeny et al., 2002). Moreover, the use of genetically-modified MSCs may represent an efficient alternative therapy capable of circumventing limitations associated with the systemic administration of some cytokines and drugs such as short half-life and toxicity (Fritz and Jorgensen, 2008). Recent advances in the field of gene therapy have generated heightened expectations regarding the improvement of treatment for advanced malignancies, including melanoma (Komenaka et al., 2004; Rietschel and Chapman, 2006). The cytokine interferon-beta (IFN-β) is known to have potent pro-apoptotic effects and is capable of inhibiting both tumor growth and angiogenesis (Chawla-Sarkar et al., 2001; Jonasch and Haluska, 2001; Kirkwood and Ernstoff, 1984). Several reports indicate that mesenchymal stem cells engineered to secrete IFN-β trafficked to and reduced the tumor burden of melanoma, breast carcinoma, prostate cancer, and lung metastases (Ren et al., 2008; Studeny et al., 2002; Studeny et al., 2004b). Here, it was investigated whether greater reduction of the tumor

burden could be achieved by using targeted delivery of canine AT-MSCs (cAT-MSC) expressing IFN-β in combination with a low dose cisplatin (*cis*-diamminedichloroplatinum) protocol. Cisplatin is one of the most potent chemotherapeutic agents; unfortunately, it also often has significant gastrointestinal toxicities, nephrotoxicities, and hematological side effects (Loehrer and Einhorn, 1984). However, the side effects of this drug are substantially reduced at a lower dose. It has been reported that the combination of IFN-β cytokine therapy with anti-cancer drugs synergistically suppressed the cell growth of hepatocellular carcinoma and melanoma (Damdinsuren et al., 2003). Based upon this observation, it was hypothesized that cAT-MSC-mediated targeted delivery of IFN-β might demonstrate a synergistic anti-tumor effect if combined with low dosage cisplatin.

This study present evidence of a significant tumor suppression by cAT-MSC alone on canine melanoma (LMeC) *in vitro* and *in vivo* which was enhanced further when cAT-MSC expressed IFN-β. In addition, the effects of stem cell-mediated gene delivery of IFN-β were investigated in combination with systemic treatment with low doses of cisplatin in a canine malignant melanoma xenograft model; it was found that this treatment combination resulted in a significant additive anti-tumor effect.

2. Materials and methods

2.1. Cell isolation and culture

Canine adipose tissue-derived mesenchymal stem cells (cAT-MSCs) were isolated using modified methods previously described (Gimble and Guilak, 2003; Neupane et al., 2008). Briefly, adipose tissue was collected from subcutaneous fat depots of Beagle dogs using standard surgical procedures. Each adipose tissue was digested overnight at 37℃ with collagenase type IA (1 mg/mL; Sigma-Aldrich, St Louis, MO, USA) and then washed in phosphate-buffered saline (PBS). Following centrifugation, the pellet was filtered through a 100-μm nylon mesh and incubated overnight in Dulbecco's Modified Eagle's Medium (DMEM; Hyclone, Logan, UT, USA) supplemented with 10%, heat-inactivated fetal bovine serum (FBS; Hyclone) at 37℃ in a humidified atmosphere of 5% CO_2. After 24 h, non-adherent cells were removed by washing with PBS. The cell medium was then changed to K-NAC medium, which is a modified MCDB 153 medium (Keratinocyte-SFM; Invitrogen, Carlsbad, CA, USA) supplemented with 2 mM N-acetyl-L-cysteine (NAC; Sigma-Aldrich) and 0.2 mM L-ascorbic acid 2-phosphate (Asc 2P; Sigma-Aldrich). This medium contained 0.09 mM calcium, 5 ng/mL human recombinant epidermal growth factor (rEGF; Invitrogen), 50 μg/mL bovine pituitary extract (BPE; Invitrogen), 5 μg/mL

insulin (Sigma-Aldrich) and 74 ng/mL hydrocortisone (Sigma-Aldrich). The medium was changed at 48-h intervals until the cells became confluent. When cells were >90% confluent, they were banked or serially subcultured under standard conditions. Before their use in the experiments, MSCs were identified based on the following cell surface markers: $CD73^{hi}$, $CD90^{hi}$, $CD31^{-}$, and $CD45^{-}$. The cAT-MSCs were maintained in DMEM supplemented with 10%, heat-inactivated FBS and 1X Pen/Strep (Invitrogen, CA, USA) at 37℃ in a humidified atmosphere of 5% CO_2. Canine AT-MSC preparation was performed under GMP (Good Manufacturing Practice) conditions (RNL BIO). LMeC, a canine melanoma cell line derived from metastatic mandibular lymph node of canine oral melanoma (Inoue et al., 2004) was maintained in DMEM (Hyclone), supplemented with 10% FBS and 1X Pen/Strep at 37℃ in a humidified atmosphere of 5% CO_2.

2.2. Construction of lentiviral vectors and transduction of cAT-MSC

The lentiviral vector carrying the canine interferon beta gene (cIFN-β) was generated as described previously (Seo et al., 2011a). Briefly, the target gene amplified by PCR from canine thymus cDNA was cloned into the pLenti6/V5-D-TOPO® vector using the pLenti/V5 Directional TOPO Cloning Kit (Invitrogen). The resulting lentiviral vector carrying IFN-β was sequenced to verify the correct reading frame and DNA sequence.

Lentivirus particles were amplified in 293FT cells using the ViraPower™ Lentiviral Expression System (Invitrogen) according to the manufacturer's protocol.

For transduction, the viral supernatant was added to cAT-MSC at a multiplicity of infection of 5 with 6 μg/mLPolybrene (Sigma-Aldrich). After 16 h, the medium was replaced with fresh DMEM with 10% FBS. After an additional 24 h, the cells were cultivated in selection medium containing 5 μg/mL blasticidin (Invitrogen) for 5 days. The cells were prepared routinely and used for *in vitro* and *in vivo* studies as low-passage cultures (passages 4-6) (Ren et al., 2008).

Successful transduction of the cAT-MSC-IFN-β cells was confirmed by reverse transcription-PCR. The sense and antisense primers of each primer pair were designed to bind to different exons to exclude DNA contamination: canine IFN-β (sense 5'-GAGAGGATCCAATGACCAGTAGATGCATCCT-3', antisense 5'-ATTTGATGTTGGCGGGAT-3', 561 bp amplicon). Total RNA was extracted with easy-BLUE™ Total RNA Extraction kit (iNtRON Bio., Seoul, Korea). Complementary DNA templates from each sample were prepared from 1 μg of total RNA primed with oligodT primer using 400 units of Moloney murine leukemia virus reverse transcriptase (M-Mulv RT) (Invitrogen), followed by 30 PCR amplification cycles (94℃ for 30 s, annealing at 57℃ for 30 s, and extension at 72℃ for 90 s). Glyceraldehyde-3-phosphate dehydrogenase (GAPDH) was used as the reaction standard:

sense 5'-GGTCACCAGGGCTGCTTT-3', antisense 5'-ATTTGATGTTGGCGGGAT-3', 209 bp amplicon, 25 PCR amplification cycles). Each PCR product was analyzed by 1.5% agarose gel electrophoresis.

2.3. IFN-β ELISA assay

The amount of IFN-β secreted by cAT-MSC-IFN-β into the media was quantified by a canine IFN-β enzyme-linked immunosorbent assay (ELISA) kit (BlueGene Biotech, Shanghai, China). cAT-MSC-IFN-β cells were plated at 1 x 10^5 cells per well in 12-well plates. After 24, 48 and 72 h, the IFN-β level in the medium was determined according to manufacturer's protocols using recombinant IFN-β as a standard (Rachakatla et al., 2007). Assays were performed in triplicate.

2.4. *In vitro* migration assay

The propensity of cAT-MSCs to migrate towards LMeC melanoma cells was evaluated using a modified 24-well-transwell migration assay. LMeC cells (10^5 cells/mL) were incubated in serum-free DMEM for 24 h, conditioned medium was collected and placed in the lower wells of the transwell plates. Serum-free medium without any cells served as a negative

control and medium supplemented with 10% FBS was used as a positive control. The cAT-MSC-Mock (empty vector-transduced cAT-MSC) or cAT-MSC-IFN-β (5 x 10^4/250 µL) in serum-free medium were seeded onto transwell inserts (8 µm; BD Falcon) coated with gelatin (10 µL of 0.5 mg/mL). After incubation for 12 h at 37℃, the nonmigrating cells were removed from the upper surface of the transwell membrane using a cotton swab. The membranes were fixed and stained using 1% crystal violet (Sigma-Aldrich) in 4% Paraformaldehyde for 1 min and washed in distilled water. Nuclei of the migratory cells were counted in five high-power fields (x200). Results were expressed as the percentage of controls (cells migrating toward serum-free medium) (mean ± SD); all experiments were conducted in triplicate. The statistical significance in mean values among multiple sample groups was examined with two-way ANOVA and Bonferroni's *post-hoc* test using GraphPad Prism (version 4) software (Graphpad Software Inc., San Diego, CA, USA). Differences between two conditions at $p<0.05$ were considered statistically significant.

2.5. Direct co-culture of LMeC melanoma cells with cAT-MSC *in vitro*

LMeC melanoma cells (3 x 10^3 cells) were cultured either alone or mixed with 1.5 x 10^3 cells of cAT-MSC-Mock or cAT-MSC-IFN-β (ratio of tumor

cells : cAT-MSCs was 2:1) on four-well chamber slides (Lab-Tek, Naperville, IL, USA) for 72 h. cAT-MSC-Mock and cAT-MSC-IFN-β cells were labeled with red fluorescent dye, CM-DiI (Molecular Probes, Eugene, OR, USA) before co-culture with LMeC cells. After incubation, LMeC cells and cAT-MSCs were stained with Hoechst 33342 (Lonza, Basel, Switzerland) to visualize the nuclei, and examined with a fluorescence microscopy Olympus BX41 microscope (Tokyo, Japan).

For flow cytometry (FACS) analysis, LMeC cells (1 x 10^5 cells) were plated in 60-mm culture plates alone or mixed with cAT-MSC-Mock or cAT-MSC-IFN-β, respectively, at a ratio of 2 LMeC cells to 1 cAT-MSC-Mock or cAT-MSC-IFN-β. After 3 days, the cells were trypsinized, counted, and fixed with 70% ethanol. For analysis of DNA content, the cells were labeled with propidium iodide (Sigma-Aldrich) in the presence of RNase A (Sigma-Aldrich) (50 g/mL, 30 min, 37℃ in the dark) (Studeny et al., 2004b). Samples were run on a FACScan flow cytometer (Becton-Dickinson, FL, NJ, USA), and data were analyzed using FCS Express 4 (De Novo Software, Thornhill, Ontario, Canada). Results were expressed as the percentage of control cell growth: (the number of tumor cells co-cultured with cAT-MSC-Mock or with cAT-MSC-IFN-β on day 3 – the number of tumor cells co-cultured on day 0/(the number of tumor cells cultured alone on day 3 – number of tumor cells cultured alone on day 0) x 100. The values were expressed as means ± SD. The statistical significance in mean values was

examined with Bonferroni's multiple comparisons test after one-way ANOVA test.

2.6. Indirect co-culture of LMeC melanoma cells with cAT-MSC and cell cycle analysis

A quantity of 5×10^4 LMeC cells were plated on 6-well plate and 5×10^4 or 2×10^5 cells of cAT-MSC β (the ratio tumor cells : cAT-MSCs was 1:1 or 1:4) were placed in transwell inserts (0.4 μm pore size; BD Falcon, Franklin Lakes, NJ). Inserts with cAT-MSC-Mock or cAT-MSC-IFN-β were transferred into wells with LMeC cells after 24 h of culture. After 3 days, the cells were trypsinized, counted, and fixed with 70% ethanol. For cell-cycle analysis, the cells were labeled with propidium iodide in the presence of RNase A (50 g/mL, 30 min, 37℃ in the dark), and resuspension in PBS. Samples were run on a FACScan flow cytometer and the data were analyzed by using FCS Express 4. The results were the means (± SD) of three independent experiments. The statistical significance in mean values was examined with Bonferroni's multiple comparisons test after one-way ANOVA test.

2.7. Evaluation of the effect of cAT-MSC-IFN-β on the growth of LMeC xenografts

Five-week-old female BALB/c nude mice (20-30 g) were purchased from Central Lab. Animal, Inc. (Seoul, Republic of Korea). All animals were handled in strict accordance with the recommendations in the Guide for the Care and Use of Laboratory Animals of the National Institutes of Health. The mice study was approved by the Seoul National University Institutional Animal Care and Use Committee (Permit Number: SNU-110609-1). Mice were held for 1 week after arrival to allow them to acclimate. To induce canine melanoma tumor development in the animals, LMeC cells (5×10^6) suspended in 200 μL PBS were injected subcutaneously (SC) into the flanks of mice. When tumors with a 5 to 6 mm diameter had developed, mice were randomly separated into five groups (n=4/group), with each group receiving one of the following (Figure 7): Group 1 was given intraperitoneal, low dose cisplatin (2 mg/kg), group 2 was given circumtumoral cAT-MSC-Mock cells (5×10^5/100 μL PBS), group 3 was given circumtumoral cAT-MSC-IFN-β cells (5×10^5/100 μL PBS), group 4 was given a combination of intraperitoneal cisplatin (2 mg/kg) and circumtumoral cAT-MSC-IFN-β cells (5×10^5/100 μL PBS), and group 5 was given circumtumoral PBS as a control. Three days after initiation of single drug treatment (PBS or cisplatin) cAT-MSC-Mock or cAT-MSC-IFN-β or PBS was administered 3 times at 3 days interval in respective treatment groups. The size of each tumor mass was measured every 3 days with a vernier caliper (Mitutoyo, Tokyo, Japan);

tumor volume was calculated using the following formula: tumor volume (mm^3) = (a^2 x b)/2, where a is the length of the short axis and b is the length of the long axis. The values were expressed as means ± SD. The statistical significance in mean values among multiple sample groups was examined with Newman-Keuls multiple comparisons test after one-way ANOVA test. Mice were euthanized when the tumors reached 3000 mm^3 in volume (< 10% of body weight), or as soon as tumors showed signs of necrosis, ulceration, or bleeding. Mice were killed by lethal exposure to CO_2 followed by cervical dislocation.

2.8. Tissue processing and imaging of transplanted cAT-MSCs

Homing of cAT-MSC to tumor tissue *in vivo* was determined by fluorescence microscopy analysis of cAT-MSC labeling with the red fluorescent dye, CM-DiI, before *in vivo* administration. Cultured cAT-MSCs were trypsinized and resuspended at a concentration of 1 x 10^6 cells per 2 μg of CM-DiI dye in 1 mL of Dulbecco's PBS and labeled by incubation for 5 min at 37℃. Unincorporated dye was washed away with PBS then CM-DiI labeled cells were injected subcutanously to mice exhibiting tumor formation. Three days after the last injection, mice were sacrificed and tumor tissue was harvested and fixed in 4% paraformaldehyde. Tumor tissue from each group of mice was embedded in Tissue Tek OTC compound

(Sakura Finetek, CA, USA), snap-frozen in liquid nitrogen, and stored at -80℃. Frozen tissue was sectioned (7-µm-thick sections), mounted onto slides, and stained with Hoechst 33342. Images were captured with the use of a fluorescence microscope (IX 71, Olympus, Japan) equipped with a digital camera (DP71, Olympus) and processed using Image J software 1.45s version (National Institutes of Health, USA).

2.9. TUNEL assay

Apoptotic cells in tumor tissue were identified using a TUNEL (terminal deoxynucleotidyl transferase-mediated nick-end labeling) assay (In Situ Cell Death Detection Kit, Fluorescein; Roche Diagnostics GmbH, Mannheim, Germany) according to the manufacturer's instructions. The 7-µm-thick frozen tissue sections were fixed with 4% paraformaldehyde for 20 min at room temperature followed by the addition of permeabilization solution (0.1% Triton X-100, 0.1% sodium citrate) for 2 min at 4℃. Labeling of DNA was done by treating the slides with 25 µL of TUNEL reaction mixture for 1 h at 37℃ in a humidified chamber in the dark. The slides washed thrice in PBS and then the TUNEL-positive cells were analyzed under a fluorescence microscope.

3. Results

3.1. Confirmation of IFN-*β* expression from cAT-MSC-IFN-*β*

cAT-MSCs were transduced with the canine IFN-*β*-expressing plasmid pLenti/V5 and its expression was confirmed by reverse transcription-PCR and ELISA. IFN-*β* mRNA expression was detected by RT-PCR, which showed positive expression only in cAT-MSC-IFN-*β* (Figure 8A). The resulting IFN-*β* protein expression was determined by ELISA and the cultured cAT-MSC-IFN-*β* supernatant contained a significantly greater amount of IFN-*β* protein compared with cAT-MSC control (Figure 8B). After 48 h of incubation, the canine IFN-*β* concentration produced by cAT-MSC-IFN-*β* was found to be 344.82 pg/mL or approximately 3.5×10^{-3} pg per cell. cAT-MSC-Mock cells had less than 5 pg/mL IFN-*β* protein expression.

3.2. Migratory capability of cAT-MSC-IFN-*β in vitro*

MSCs are intrinsically tropic for tumor cells which is central to their utility as a reliable delivery vehicle for cancer gene therapy (Kim et al., 2006). The *in vitro* tumor-tropic properties of cAT-MSC-Mock and cAT-MSC-IFN-*β* to LMeC cells were evaluated using a modified transwell

migration assay (Figure 9A and 9B). LMeC conditioned medium (CM) significantly stimulated migration of cAT-MSC-Mock and cAT-MSC-IFN-β as compared with negative control medium ($p<0.01$; Figure 9B). These two stem cell lines demonstrated significant migratory capabilities toward LMeC conditioned medium; however, there was no significant difference in migration ability toward LMeC CM between the cAT-MSC-Mock and cAT-MSC-IFN-β cell types.

3.3. Inhibition of LMeC growth by cAT-MSC-Mock and cAT-MSC-IFN-β *in vitro*

To investigate whether cAT-MSC-IFN-β cells have an inhibitory effect on LMeC cell growth and viability, LMeC cells were cultured at a 2:1 ratio with CM-DiI-labeled cAT-MSC-Mock or cAT-MSC-IFN-β in a direct co-culture system (3×10^3 LMeC to 1.5×10^3 cAT-MSC-IFN-β). LMeC cells and cAT-MSCs stained by Hoechst, were observed by fluorescence microscopy (Figure 10A). As shown in Figure 10A, cAT-MSC-IFN-β directly inhibited the growth of LMeC cells as compared with LMeC cells alone. To evaluate the growth inhibitory effect of cAT-MSC-IFN-β on LMeC cells more accurately, cells were counted and the relative numbers of aneuploid tumor cells and diploid cAT-MSCs in the co-cultures were determined by flow cytometry (Figure 10B and 10C). After 72h, the number

of LMeC cells after co-culture with cAT-MSC-Mock or cAT-MSC-IFN-β had increased to 10.34 ± 1.73 x 10^5 and 8.40 ± 0.55 x 10^5 cells, respectively. In comparison, the number of LMeC cells in the control group (LMeC alone) had increased to 11.93 ± 1.62 x 10^5 cells. These data indicate that cAT-MSC-IFN-β can directly inhibit the growth of malignant tumor cells as compared to control (67.76% of control growth, $p<0.05$, Figure 10C), albeit in the absence of the host immune system. LMeC proliferation was slightly inhibited by co-culture with cAT-MSC-Mock, but the difference was not statistically significant (85.40% of control growth, Figure 10C).

Similarly, when cAT-MSC-IFN-β and LMeC cells were co-cultured but separated by a transwell membrane, which allows the exchange of soluble factors but prevents direct cell-to-cell contact, LMeC proliferation was again significantly reduced (Figure 11). The number of LMeC cells present after treatment with cAT-MSC-IFN-β was 9.85 ± 1.31 x 10^5 (1:1 ratio, 73.23% of control growth, $p<0.01$) and 7.32 ± 0.81 x 10^5 (1:4 ratio, 45.15% of control growth, $p<0.001$), respectively. In comparison, the number of LMeC cells in the control group was 13.45 ± 0.66 x 10^5 (1:1) and 16.23 ± 1.04 x 10^5 (1:4), respectively. The number of LMeC cells present after treatment with cAT-MSC-Mock was 11.5 ± 1.25 x 10^5 (1:1 ratio, 85.5% of control growth, $p>0.05$) and 12.88 ± 0.59 x 10^5 (1:4 ratio, 79.35% of control growth, $p<0.001$), respectively. The proliferation of LMeC cells was inhibited significantly when co-cultured with either cAT-MSC-IFN-β or with cAT-

MSC-Mock (at a cAT-MSC/LMeC ratio of 4:1). Therefore, expression of cAT-MSC-IFN-β exhibited potent dose-dependent inhibitory effects on LMeC cell proliferation.

3.4. Effect of cAT-MSC-IFN-β on cell cycle distribution of LMeC

Flow cytometric cell cycle analysis showed that the proportion G0/G1 phase LMeC cells co-cultured with cAT-MSC-IFN-β at a ratio of 1 MSC to 1 LMeC cell, was higher than that of the controls ($p<0.05$, Figure 12A and 12B). LMeC cells co-cultured with cAT-MSC-IFN-β at a ratio of 4 MSCs to 1 LMeC cell, showed increases in the G0/G1 phase of the cell cycle compared to the controls ($p<0.01$, Figure 12C and 12D). G1 arrest occurred concurrently with a reduction in the percentage of S phase cells ($p<0.01$ and $p<0.001$ at a cAT-MSC-IFN-β/LMeC ratio of 1:1 and 4:1 respectively, Figure 12B and 12D). LMeC cells co-cultured with cAT-MSC-Mock also exhibited a decrease in S phase as compared to the controls ($p<0.05$ and $p<0.05$ at a cAT-MSC/LMeC ratio of 1:1 and 4:1 respectively, Figure 12B and 12D). LMeC co-cultured with cAT-MSC-Mock exhibited a slight increase in the percentage of cells in G2/M phase as compared to controls ($p<0.05$ at a cAT-MSC/LMeC ratio of 4:1). These results show that cAT-MSC-Mock and cAT-MSC-IFN-β may prevent the normal progression of the tumor cell cycle.

3.5. Effect of combination treatment of cAT-MSC-IFN-*β* and cisplatin on LMeC tumors *in vivo*

To evaluate the antitumor effects of cAT-MSC-IFN-*β* combined with cisplatin on canine melanoma cells *in vivo*, LMeC cell xenografts were established in female BALB/C nude mice. Melanoma tumors were grown in nude mice by subcutaneous injections of LMeC cells into the flank. Control tumors grew rapidly, averaging 1620.4 ± 298.4 mm^3 in size by 39 days following initiation of treatment (Figure 13). In contrast, tumor volumes were significantly reduced in all groups that received either cisplatin (1000.8 ± 72.6 mm^3, $p<0.001$), cAT-MSC-Mock (777.4 ± 84.0 mm^3, $p<0.001$), cAT-MSC-IFN-*β* (421.1 ± 102.1 mm^3, $p<0.001$), or both cisplatin and cAT-MSC-IFN-*β* cells (157.7 ± 98.7 mm^3, $p<0.001$), in comparison with mice that received PBS as a control (Figure 13A and 13B). cAT-MSC-IFN-*β* produced a significantly greater tumor growth inhibition compared to cAT-MSC-Mock ($p<0.01$). Combining cAT-MSC-IFN-*β* with cisplatin produced a significantly greater tumor growth inhibition compared to cisplatin alone ($p<0.001$), cAT-MSC-Mock ($p<0.001$) or cAT-MSC-IFN-*β* alone ($p<0.05$). These data demonstrate that combination treatment can reduce the tumor volume more effectively than monotherapy.

3.6. Transplanted cAT-MSCs migrate to melanoma tumor region

To track the homing of transplanted cAT-MSC-IFN-β to tumor cells in the canine melanoma model, cAT-MSC-IFN-β cells were labeled with the cell tracker dye CM-DiI before *in vivo* administration. Three days after the last administration of cAT-MSCs in mice, the tissues were harvested and frozen tumor sections were made. Fluorescent microscopic analysis of tumor section provided evidence for homing of cAT-MSC-IFN-β (red fluorescence) to the tumor site as shown in Figure 14A. Therefore, cAT-MSC-IFN-β has tumor-tropic properties and localizes to melanoma tumor tissue where it exerts its therapeutic activity by producing IFN-β.

3.7. Evaluation of tumor cell apoptosis by TUNEL assay

The induction of cell apoptosis in tumor tissues treated by each treatment group was evaluated by TUNEL assay (Figure 14B). Three days after the last injection of cAT-MSCs, representative tumors were harvested from each group and frozen tumor sections were made for subsequent apoptosis analyses. Combination treatment with cAT-MSC-IFN-β plus cisplatin resulted in a greater apoptotic response of cells than in the other treatment groups, indicating that enhancement of the apoptotic response may be contributing to the additive effect.

4. Discussion

Conventional cytotoxic chemotherapy has been the mainstay of medical treatment for a variety of tumor types. However, clinical applications of chemotherapeutic agents are often limited by their dose-dependent toxicities and drug resistances (Kitchell et al., 1994). Over the past decades, researchers have attempted to identify novel approaches to achieve more efficient melanoma therapies (Whitley et al., 1995). Although some therapies have reported promising preclinical results, clinical trials involving single-agent therapies have not indicated much benefit for patients' overall survival (Pópulo et al., 2012). In this report, additive effects could be achieved by a combination of stem cell-based gene therapy and chemotherapy in canine malignant melanoma. cAT-MSCs selectively engraft in melanoma tissue, can be engineered to secrete a therapeutic protein, IFN-β, and can significantly reduce tumor burden in an animal model. This is the first report to demonstrate the efficacy of combining a systemic chemotherapy with stem-cell-based, targeted delivery of a cytokine to a malignant canine melanoma in the athymic nude mouse.

cAT-MSC expressing canine IFN-β was constructed using a lentiviral vector system, which offers the potential for long-term gene expression. AT-MSCs are considered to be a promising source of cellular vehicles for targeted cancer gene therapy (Ren et al., 2008; Studeny et al., 2002). AT-

MSCs have an intrinsic tumor tropism and can thus facilitate the local production of tumoricidal therapeutic agents within the tumor microenvironment. Previously, it was confirmed that lentivirus-transduced cAT-MSC expressed the cell surface marker phenotype characteristic of AT-MSCs (Wagner et al., 2005). Indeed, flow cytometric analyses confirmed that cAT-MSC were positive for CD29, CD73, CD90, CD44 and CD105 yet lacked detectable CD31 and CD45 (unpublished data).

Next, it was demonstrated the capability of cAT-MSC to actively migrate toward the tumor *in vitro* and *in vivo*. Both cAT-MSC-IFN-β as well as cAT-MSC-Mock demonstrated significant directional migratory capabilities toward LMeC cells, suggesting that the migration activity of cAT-MSCs was not influenced by lentiviral-vector-mediated genetic modification and IFN-β expression. The result of the migration assay also indicates that the melanoma cancer cells may contain chemoattractant factors which accelerate the migration of the cAT-MSC-Mock and cAT-MSC-IFN-β cells, thus enhancing the delivery of a therapeutic cytokine to tumors *in situ*. It has been reported that epidermal growth factor, platelet-derived growth factor, stromal cell-derived factor-1/CXCR4, SCF/c-Kit and vascular endothelial growth factor (VEGF)/VEGF receptor (VEGFR) 1 and VEGFR2 may play a role in the tumor-tropic effects (Nakamizo et al., 2005). Migratory properties of AT-MSCs should be further evaluated for tumor specificity and

possible signaling mechanisms should be investigated in preparation for possible therapeutic applications.

Despite extensive investigation over the past ten years, the impact of MSCs on tumor progression is still greatly debated. Some studies have shown that MSCs promote tumor progression and metastasis (Xu et al., 2009; Yan et al., 2012) yet other studies report that MSCs suppress tumor growth (Cousin et al., 2009; Khakoo et al., 2006; Secchiero et al., 2010). The reason for this discrepancy is unknown, but it may be attributable to differences in the experimental tumor models, the heterogeneity of MSCs preparations, the dose or timing of the MSCs injected, the animal host, or some as yet unknown factor (Klopp et al., 2011). The identification of the mechanisms involved in the interaction between stromal and cancer cells, especially the secreted factor responsible for the anti-proliferative effect of MSC is currently under investigation (Cousin et al., 2009). Inhibition of tumor growth may be mediated by high cytokine levels produced by MSCs. Other previous work has demonstrated an inhibitory effect on tumor growth mediated by MSC secretion of the Wnt-inhibitor, Dkk-1, which decreases cell cycle gene expression via the Wnt/β-catenin pathway (Qiao et al., 2008a; Thudi et al., 2011). Tumor inhibition may thus be induced by down-regulation of positive cell cycle regulators, such as cyclin D1, D2 and CDK4, along with up-regulation of the negative regulator, cyclin dependent kinase inhibitor, p27, and its subsequent inhibition of Rb phosphorylation

and G1 arrest (Torsvik and Bjerkvig, 2013). As described in this communication, cAT-MSCs reduced LMeC cell viability and proliferation in an indirect co-culture system. This observation that LMeC co-cultured with cAT-MSC-Mock exhibited a slight increase in the percentage of cells in G2/M phase as compared to controls is similar to the results reported by Ayuzawa et al (Ayuzawa et al., 2009). It was also observed that treatment with cAT-MSC-Mock reduced the tumor volume in tumor-bearing nude mice and induced an apoptotic response in tumor tissue. These results suggest that cAT-MSCs alone are capable of reducing growth of melanoma cells, perhaps by alteration of the cell cycle of cancer cells and stimulation of apoptosis.

All IFN molecules have antiviral and antiproliferative properties as well as some immunomodulatory activity. Considering both antiproliferative and anti-invasive effects of IFNs, IFN-β has the strongest anti-tumoral effect on human melanoma cells (Horikoshi et al., 1995). IFN-β may mediate anti-tumor effects either indirectly by modulating immunomodulatory and anti-angiogenic responses or directly by affecting proliferation or the cellular differentiation of tumor cells (Chawla-Sarkar et al., 2003). Despite these activities, clinical trials have failed to identify a clinical benefit for treatment with IFN-β (Einhorn and Grander, 1996). These limited clinical results may result from the short half-life and the systemic toxicities of recombinant IFN-β protein at the doses needed to achieve an antitumor effect (Einhorn

and Grander, 1996). Because a local gene therapy strategy has the potential to surmount these limitations, the effect of IFN-β gene delivery by AT-MSC has been tested. Multiple *in vitro* experiments (cell ennumeration, flow cytometry and fluorescence imaging) have been carried out in order to evaluate the anti-tumor effect of cAT-MSC-IFN-β on LMeC cells. This study has revealed that IFN-β-transduced cAT-MSC secrete significant amounts of IFN-β (Figure 8B) and inhibit the growth of cancer cells in both direct and indirect co-culture systems (Figure 9 and 10).

In this study, cAT-MSC-IFN-β have the ability to interfere with the proliferation of tumor cells by altering cell cycle progression. IFN-β can affect all phases of the mitotic cell cycle, most commonly via a block in G1 phase or, occasionally, by lengthening all phases of the cell cycle (G1, G2 and S) (Balkwill and Taylor-Papadimitriou, 1978). Although the *in vitro* apoptotic effect of cAT-MSC-IFN-β was not tested, *in vivo* data demonstrate that the treatment with cAT-MSC-IFN-β can induce an apoptotic response in tumor-bearing nude mice. These results are supported by several other studies in which IFN-β had an apoptotic and growth inhibitory effect on melanoma cells (Seo et al., 2011a; Studeny et al., 2002; Studeny et al., 2004b). Induction of apoptosis by IFN-β involved FADD/caspase-8 signaling, activation of the caspase cascade, release of cytochrome c from mitochondria, disruption of mitochondrial potential, changes in plasma

membrane integrity, and DNA fragmentation (Chawla-Sarkar et al., 2001; Chawla-Sarkar et al., 2003).

The combination of traditional chemotherapy with IFN-β has been investigated for various cancers (Choi et al., 2004; Damdinsuren et al., 2003; Hübner et al., 1995). Eugene et al. reported that the combination of adenoviral-mediated IFN gene therapy and 5-fluorouracil resulted in tumor regression, apoptosis, and improved survival in an established liver metastases model (Choi et al., 2004). The biochemical mechanism behind the synergistic effects of IFN-β with cisplatin or other chemotherapeutic agents are poorly understood. However, IFN-β is demonstrated to delay the cell cycle mainly in the S phase, which could affect the cellular uptake of chemotherapeutic agents (Damdinsuren et al., 2003). Although this study does not show a synergistic anti-tumor effect of cAT-MSC-IFN-β with cisplatin on canine melanoma cells *in vitro*, it has been previously demonstrated that the synergistic anti-tumor effects of cAT-MSC-IFN-β with cisplatin on mouse melanoma *in vitro* and *in vivo* (Seo et al., 2011a). Here, it was found that combining stem cell-based IFN-β gene therapy with cisplatin showed greater reduction in canine melanoma burden than either treatment alone. Moreover, this combination strategy could make it possible to reduce the doses of chemotherapeutic agents and their accompanying systemic toxicities. As it is likely that chemotherapy will remain a mainstay of cancer therapy for many years to come, the combination of such chemotherapeutic

agents with the stem cell-based gene therapy is likely to become an advantageous strategy.

Overall, it has been demonstrated that cAT-MSC significantly attenuate the growth of LMeC canine melanoma cells in culture and in a mouse xenograft study, and can serve as cellular vehicles for the delivery and local production of anti-tumor agent. The anti-tumor effect is increased by when cAT-MSC express IFN-β and are combined with chemotherapeutic drugs. In conclusion, the present findings provide a strong rationale for the further exploration of the combination of AT-MSC with chemotherapy in the treatment of a malignant melanoma and other tumors.

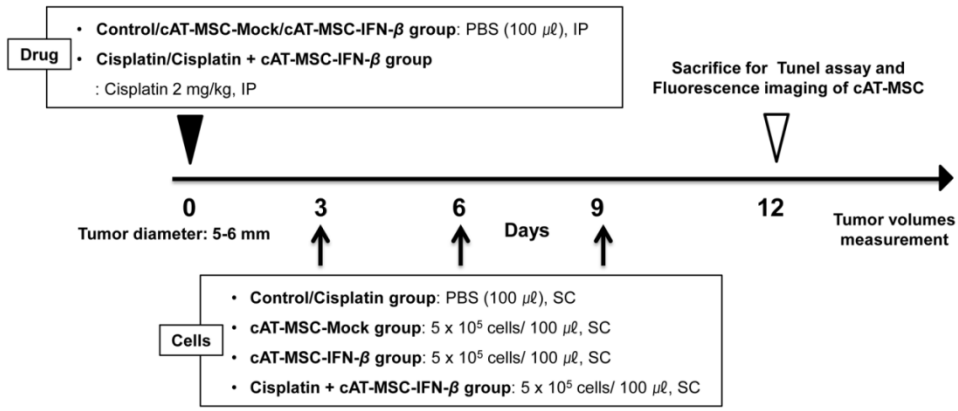

Figure 7. Time table for tumor therapy in the animal experiments.

After tumor induction with LMeC melanoma cells ($5x10^6$ cells), mice were randomly divided into five groups. The control group was treated with a circumtumoral injection of phosphate-buffered saline (PBS) (n=4). The cisplatin and combination group were treated with intraperitoneal injection of low-dose cisplatin (2 mg/kg) (n=4). The cAT-MSC-Mock, cAT-MSC-IFN-β and combination group were treated with a circumtumoral injection of each cAT-MSCs (5×10^5) in PBS 3 times at 3 days interval. The size of each mass was measured every 3 days. Three days after the last injection, mice were sacrificed and tumor tissue was harvested for fluorescence microscopy analysis.

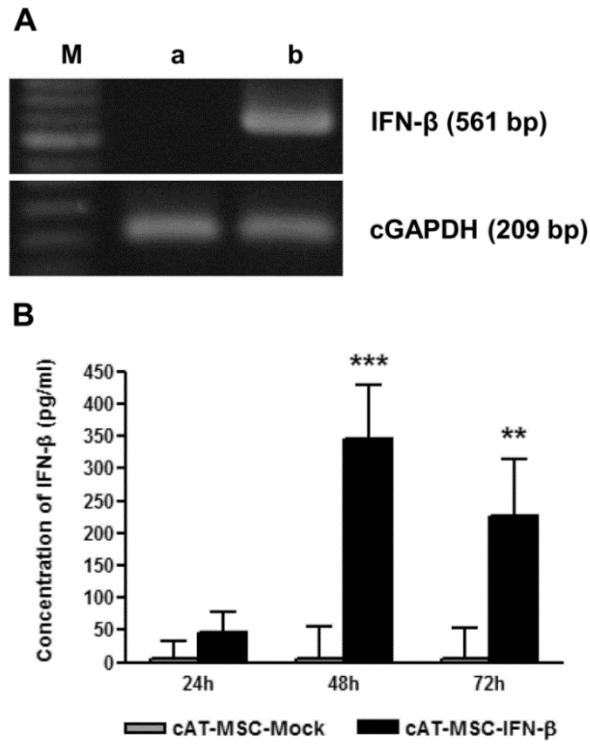

Figure 8. Confirmation of IFN-*β* expression in cAT-MSC-IFN-*β*.

(A) RT-PCR analysis of canine IFN-*β* mRNA expression in cAT-MSC-IFN-*β* compared with cAT-MSC-Mock. The expressions of canine IFN-*β* and GAPDH (cGAPDH) were detected by reverse transcriptase (RT)-PCR, and GAPDH was employed as an internal control. M, 100-bp DNA size marker; a, cAT-MSC-Mock (empty vector transducted cAT-MSC); b, cAT-MSC-IFN-*β*. (B) Canine interferon-*β* concentration (pg/mL as mean + SD) by ELISA in conditioned media harvested after 24, 48 and 72 hours in cAT-MSC-IFN-*β* compared with cAT-MSC-Mock cells; statistically significant variation between the two cell types at ** $p<0.01$ or *** $p<0.001$.

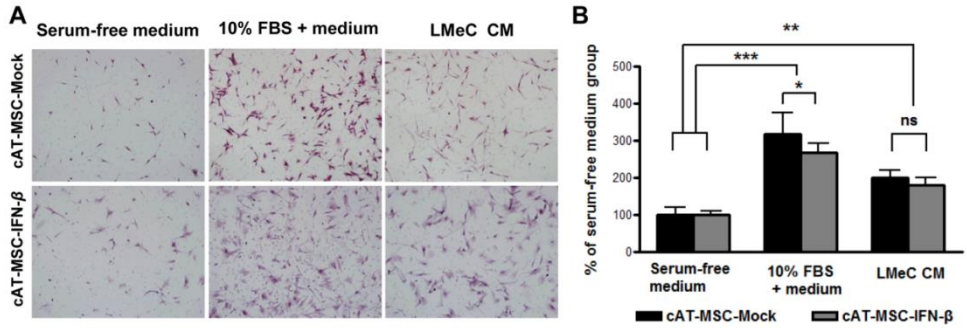

Figure 9. *In vitro* migration of cAT-MSC-Mock and cAT-MSC-IFN-*β* toward LMeC melanoma cells.

The migratory capacity of cAT-MSC-Mock and cAT-MSC-IFN-*β* were assessed by a modified transwell migration assay. LMeC cells (10^5 cells/mL) were incubated in serum-free DMEM for 24 h, conditioned medium was collected and placed in the lower wells of the transwell plates. Serum-free medium served as negative control and medium supplemented with 10% fetal bovine serum was used as a positive control. (A) Representative photographs (magnification, x200). (B) The cAT-MSC-Mock and cAT-MSC-IFN-*β* showed significant migration toward LMeC conditioned medium (CM) compared with the serum-free medium control. There was no significant difference in migration ability toward LMeC CM between cAT-MSC-Mock and cAT-MSC-IFN-*β*. Values represent the mean + SD. Data are representative of three independent experiments with similar results. * $p<0.05$, ** $p<0.01$, *** $p<0.001$

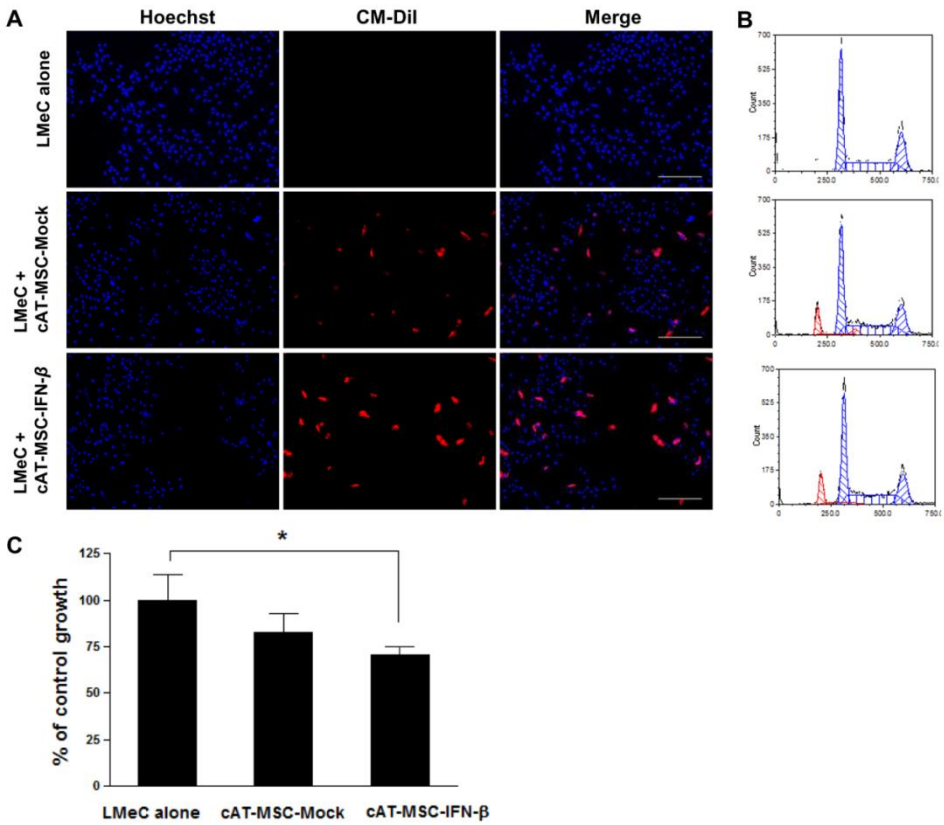

Figure 10. cAT-MSC-IFN-*β* directly inhibits the growth of LMeC melanoma cells *in vitro*.

LMeC melanoma cells were either cultured alone or co-cultured directly with CM-DiI-labeled cAT-MSC-Mock and cAT-MSC-IFN-*β* (the ratio tumor cells:cAT-MSCs was 2:1) for 72 h. (A) LMeC cells and cAT-MSCs stained by Hoechst, were examined with fluorescence microscopy. Scale bar = 100 µm. (B) Numbers of diploid MSCs (red) and aneuploid LMeC melanoma cells (blue) were determined by flow cytometry and (C) cell count. cAT-MSC-IFN-*β* directly inhibited the growth of LMeC cells as compared with LMeC cells alone. Data are expressed as the percentage of cell number and

compared with that of the control. Values represent the mean + SD. Data are representative of three independent experiments with similar results. * $p<0.05$ (Bonferroni's method for multiple comparisons).

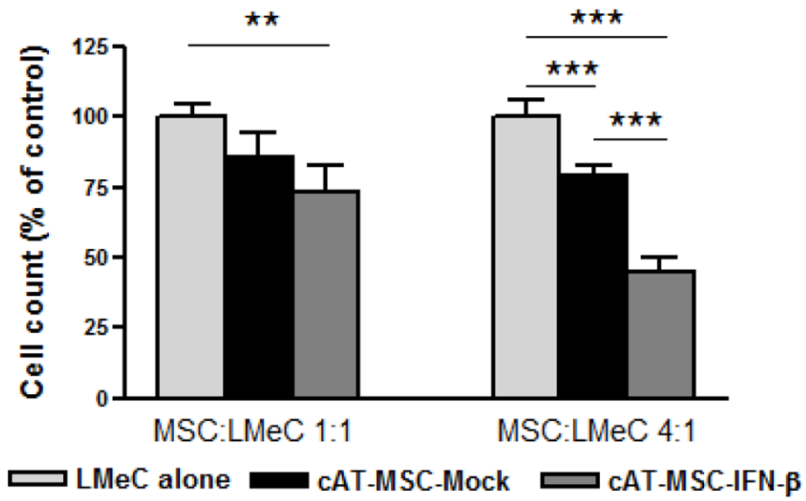

Figure 11. cAT-MSC-IFN-*β* inhibits the growth of LMeC melanoma cells in a transwell system.

LMeC melanoma cells were either cultured alone or co-cultured with cAT-MSC-Mock or cAT-MSC-IFN-*β* for 72 h in a 1:1 and 4:1 (MSC/LMeC cell) ratio. LMeC cell growth was assessed with cAT-MSCs in a transwell format, which prevented LMeC-MSC cell contact. Data are expressed as the percentage of total cells compared with that of the control. Two cAT-MSCs exhibited a potent dose-dependent inhibitory effect on LMeC cell number. The P-value was obtained using one-way ANOVA with *post-hoc* Bonferroni's multiple comparison analysis. Each data point represents the mean + SD of three independent experiments. ** $p<0.01$, *** $p<0.001$.

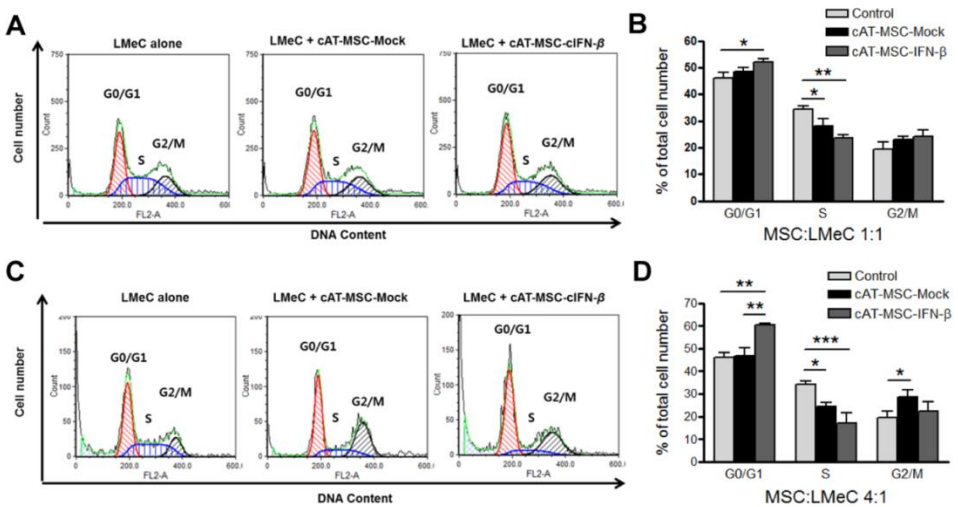

Figure 12. Cell cycle arrest of LMeC indirect co-cultured with cAT-MSC-IFN-*β*.

The cell cycle phase distribution of LMeC was analyzed after harvest by flow cytometery. (A, B) cAT-MSC:LMeC 1:1 and (C, D) 4:1. The LMeC cells co-cultured with cAT-MSC-IFN-*β,* showed increase in the G0/G1 phase of the cell cycle compared to the controls ($p<0.05$ and $p<0.01$ at a cAT-MSC-IFN-*β*/LMeC ratio of 1:1 and 4:1 respectively). G1 arrest occurred concurrently with a reduction in the percentage of S phase cells ($p<0.01$ and $p<0.001$ at a cAT-MSC-IFN-*β*/LMeC ratio of 1:1 and 4:1 respectively). The P-value was obtained using one-way ANOVA with *post-hoc* Bonferroni's multiple comparison by comparing treated cAT-MSCs (cAT-MSC-Mock or cAT-MSC-IFN-*β*) with control (LMeC alone) for each phase of the cell cycle. Data are representative of three independent experiments with similar results. * $p<0.05$, ** $p<0.01$, *** $p<0.001$

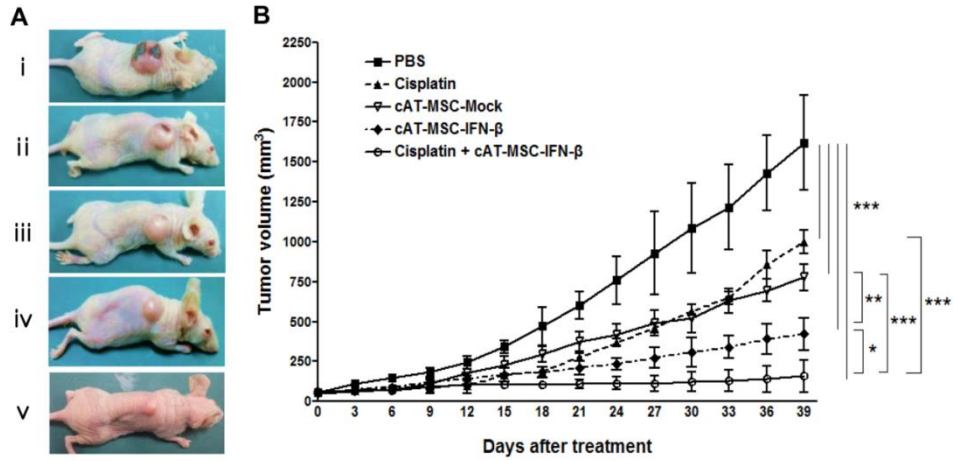

Figure 13. Growth inhibitory effects of cAT-MSC-IFN-*β* and low-dose cisplatin in a canine melanoma model.

(A) Representative tumors on day 33 in athymic nude mice: ⅰ) PBS control; ⅱ) Cisplatin (2 mg/kg); ⅲ) cAT-MSC-Mock; ⅳ) cAT-MSC-IFN-*β*; ⅴ) cAT-MSC-IFN-*β* combined with low-dose cisplatin (2 mg/kg). (B) Tumor volumes were measured in the LMeC melanoma model for the cisplatin-only, cAT-MSC-Mock-only, cAT-MSC-IFN-*β*-only and cAT-MSC-IFN-*β* combined with low-dose cisplatin (2 mg/kg). Animals (n=4/group) were divided into five groups according to treatment: cisplatin (2 mg/kg), cAT-MSC-Mock (5 x10^5 cells), cAT-MSC-IFN-*β* (5 x10^5 cells) and cAT-MSC-IFN-*β* (5 x10^5 cells) combined with cisplatin. The size of each mass was measured every three days with vernier caliper. Tumor volumes were significantly reduced in all the groups that received either cisplatin, cAT-MSC-Mock, cAT-MSC-IFN-*β*,or both cisplatin and cAT-MSC-IFN-*β* cells,

in comparison with mice that received PBS as a control. Mice that received combined treatment of cisplatin and cAT-MSC-IFN-β cells showed a greater reduction in tumor volume than the mice that received either cisplatin (p<0.001) or cAT-MSC-IFN-β cells alone (p<0.05). Data are presented as the mean ± SD, and determination of statistical significance was performed using a ANOVA analysis followed by Newman-Keuls multiple comparison test. * p<0.05, ** p<0.01, *** p<0.001

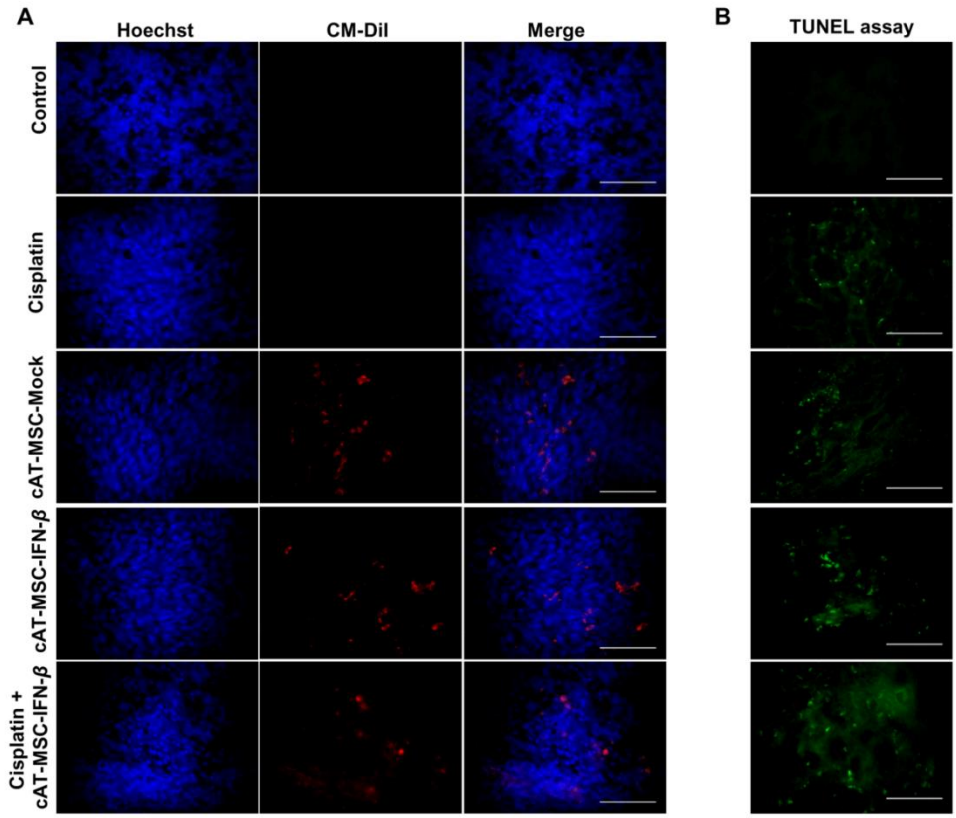

Figure 14. Fluorescence analysis of CM-DiI labeled cAT-MSC and apoptotic melanoma cells in the frozen tumor sections.

(A) Fluorescent analysis of CM-DiI labeled cAT-MSC homing to tumors in the frozen tumor sections. Subcutaneously administered CM-DiI labeled cAT-MSC-Mock or cAT-MSC-IFN-β (red) integrate into tumor lesion. Sections were counterstained with Hochest 33342 nuclear stain (blue). (B) The combination treatment of cAT-MSC-IFN-β with cisplatin results in induction of apoptosis in LMeC melanoma model. Apoptotic cells were detected using the *in situ* death detection kit Fluorescein. Tumor tissues

were harvested three days after the last injection of cAT-MSC. The combination treatment of cAT-MSC-IFN-β with cisplatin showed a greater apoptotic response than the other groups. Scale bar = 25 μm

General conclusion

The purpose of this study was to investigate the anti-tumor potential of human and canine AT-MSCs in melanomas. First, the effect of human AT-MSCs on melanoma growth was evaluated in two experimental systems. The second study was designed to determine the possibility that the combination of stem cell-based gene therapy with low-dose cisplatin would improve therapeutic efficacy against canine melanoma. The conclusions are as follows;

In the first experiment;

1. AT-MSC-CM can inhibit the proliferation of A375SM and A375P melanoma cells *in vitro*.
2. AT-MSC-CM represses cell growth via cell cycle arrest in the G0/G1 phase. Cyclin D1 levels decreased in A375SM and A375P cells treated with AT-MSC-CM, which probably indicates that AT-MSC-CM can down-regulate the cyclin D1 protein level, ultimately leading to cell cycle arrest of melanoma cell.
3. AT-MSC-CM can induce apoptosis in A375SM and A375P cell lines. AT-MSC-CM can trigger caspase-3/7 activation and, thus, PARP cleavage in melanoma cells ultimately leading to apoptosis.

4. AT-MSC-CM was found to inhibit the migration of A375SM and A375P melanoma cells.
5. When AT-MSCs were administered circumtumorally in tumor-bearing nude mice, tumor growth was inhibited.

Since AT-MSCs are easily obtained without any ethical concerns, cell therapy using AT-MSCs appears to have promise as a therapeutic option for melanoma, although further research on the clinical application of AT-MSCs is needed.

In the second experiment;

1. Canine AT-MSC expressing IFN-β was constructed using a lentiviral vector system, which offers the potential for long-term gene expression.
2. Both cAT-MSC-IFN-β as well as cAT-MSC-Mock demonstrated significant directional migratory capabilities toward LMeC cells, suggesting that the migration activity of cAT-MSCs was not influenced by lentiviral-vector-mediated genetic modification and IFN-β expression.
3. The proliferation of LMeC cells was inhibited significantly when co-cultured with either cAT-MSC-IFN-β or with cAT-MSC-Mock.

4. cAT-MSC-IFN-β have the ability to interfere with the proliferation of tumor cells by altering cell cycle progression.
5. Combining stem cell-based IFN-β gene therapy with cisplatin showed greater reduction in a canine malignant melanoma xenograft model than either treatment alone.

In conclusion, the present findings provide a strong rationale for the further exploration of the combination of AT-MSC with chemotherapy in the treatment of a malignant melanoma and other tumors.

References

Abdel aziz, M.T., El Asmar, M.F., Atta, H.M., Mahfouz, S., Fouad, H.H., Roshdy, N.K., Rashed, L.A., Sabry, D., Hassouna, A.A., and Taha, F.M. (2011). Efficacy of mesenchymal stem cells in suppression of hepatocarcinorigenesis in rats: possible role of Wnt signaling. J Exp Clin Cancer Res *30*, 49.

Al-Khaldi, A., Eliopoulos, N., Martineau, D., Lejeune, L., Lachapelle, K., and Galipeau, J. (2003). Postnatal bone marrow stromal cells elicit a potent VEGF-dependent neoangiogenic response in vivo. Gene Ther *10*, 621-629.

Ame-Thomas, P., Maby-El Hajjami, H., Monvoisin, C., Jean, R., Monnier, D., Caulet-Maugendre, S., Guillaudeux, T., Lamy, T., Fest, T., and Tarte, K. (2007). Human mesenchymal stem cells isolated from bone marrow and lymphoid organs support tumor B-cell growth: role of stromal cells in follicular lymphoma pathogenesis. Blood *109*, 693-702.

Armstrong, C.A., Botella, R., Galloway, T.H., Murray, N., Kramp, J.M., Song, I.S., and Ansel, J.C. (1996). Antitumor effects of granulocyte-macrophage colony-stimulating factor production by melanoma cells. Cancer Res *56*, 2191-2198.

Ayuzawa, R., Doi, C., Rachakatla, R.S., Pyle, M.M., Maurya, D.K., Troyer, D., and Tamura, M. (2009). Naive human umbilical cord matrix derived stem cells significantly attenuate growth of human breast cancer cells in vitro and in vivo. Cancer Lett *280*, 31-37.

Bae, J.M., Kim, H.O., and Park, Y.M. (2009). Progression from Acral Lentiginous Melanoma in situ to Invasive Acral Lentiginous Melanoma. Annals of dermatology *21*, 185-188.

Balch, C.M., Gershenwald, J.E., Soong, S.J., Thompson, J.F., Atkins, M.B., Byrd, D.R., Buzaid, A.C., Cochran, A.J., Coit, D.G., Ding, S., *et al.* (2009). Final version of 2009 AJCC melanoma staging and classification. J Clin Oncol *27*, 6199-6206.

Balkwill, F., and Taylor-Papadimitriou, J. (1978). Interferon affects both G1 and S+G2 in cells stimulated from quiescence to growth. Nature *274*, 798-800.

Belmar-Lopez, C., Mendoza, G., Oberg, D., Burnet, J., Simon, C., Cervello, I., Iglesias, M., Ramirez, J.C., Lopez-Larrubia, P., Quintanilla, M., *et al.* (2013). Tissue-derived mesenchymal stromal cells used as vehicles for anti-tumor therapy exert different in vivo effects on migration capacity and tumor growth. BMC Med *11*, 139.

Blackwood, L., and Dobson, J.M. (1996). Radiotherapy of oral malignant melanomas in dogs. J Am Vet Med Assoc *209*, 98-102.

Boria, P.A., Murry, D.J., Bennett, P.F., Glickman, N.W., Snyder, P.W., Merkel, B.L., Schlittler, D.L., Mutsaers, A.J., Thomas, R.M., and Knapp, D.W. (2004). Evaluation of cisplatin combined with piroxicam for the treatment of oral malignant melanoma and oral squamous cell carcinoma in dogs. J Am Vet Med Assoc *224*, 388-394.

Brockley, L.K., Cooper, M.A., and Bennett, P.F. (2013). Malignant melanoma in 63 dogs (2001-2011): the effect of carboplatin chemotherapy on survival. N Z Vet J *61*, 25-31.

Chawla-Sarkar, M., Leaman, D.W., and Borden, E.C. (2001). Preferential Induction of Apoptosis by Interferon (IFN)-β Compared with IFN-α2. Clin Cancer Res *7*, 1821-1831.

Chawla-Sarkar, M., Lindner, D.J., Liu, Y.F., Williams, B.R., Sen, G.C., Silverman, R.H., and Borden, E.C. (2003). Apoptosis and interferons: Role of interferon-stimulated genes as mediators of apoptosis. Apoptosis *8*, 237-249.

Chen, Q., Cheng, P., Song, N., Yin, T., He, H., Yang, L., Chen, X., and Wei, Y. (2012). Antitumor activity of placenta-derived mesenchymal stem cells producing pigment epithelium-derived factor in a mouse melanoma model. Oncology letters *4*, 413-418.

Choi, E.A., Lei, H., Maron, D.J., Mick, R., Barsoum, J., Yu, Q.-c., Fraker, D.L., Wilson, J.M., and Spitz, F.R. (2004). Combined 5-Fluorouracil/Systemic Interferon-β Gene Therapy Results in Long-Term Survival in Mice with Established Colorectal Liver Metastases. Clin Cancer Res *10*, 1535-1544.

Choi, E.W., Shin, I.S., Lee, H.W., Park, S.Y., Park, J.H., Nam, M.H., Kim, J.S., Woo, S.K., Yoon, E.J., Kang, S.K., *et al.* (2011). Transplantation of CTLA4Ig gene-transduced adipose tissue-derived mesenchymal stem cells reduces inflammatory immune response and improves Th1/Th2 balance in experimental autoimmune thyroiditis. J Gene Med *13*, 3-16.

Clarke, M.R., Imhoff, F.M., and Baird, S.K. (2014). Mesenchymal stem cells inhibit breast cancer cell migration and invasion through secretion of tissue inhibitor of metalloproteinase-1 and -2. Mol Carcinog.

Cohen, G.M. (1997). Caspases: the executioners of apoptosis. Biochem J *326 (Pt 1)*, 1-16.

Cousin, B., Ravet, E., Poglio, S., De Toni, F., Bertuzzi, M., Lulka, H., Touil, I., Andre, M., Grolleau, J.L., Peron, J.M., *et al.* (2009). Adult stromal cells derived from human adipose tissue provoke pancreatic cancer cell death both in vitro and in vivo. PLoS One *4*, e6278.

da Silva Meirelles, L., Chagastelles, P.C., and Nardi, N.B. (2006). Mesenchymal stem cells reside in virtually all post-natal organs and tissues. J Cell Sci *119*, 2204-2213.

Dai, L.-J., Moniri, M.R., Zeng, Z.-R., Zhou, J.X., Rayat, J., and Warnock, G.L. (2011). Potential implications of mesenchymal stem cells in cancer therapy. Cancer Lett *305*, 8-20.

Damdinsuren, B., Nagano, H., Sakon, M., Kondo, M., Yamamoto, T., Umeshita, K., Dono, K., Nakamori, S., and Monden, M. (2003). Interferon-β is more potent than interferon-α in inhibition of human hepatocellular carcinoma cell growth when used alone and in combination with anticancer drugs. Ann Surg Oncol *10*, 1184-1190.

Dasari, V.R., Kaur, K., Velpula, K.K., Gujrati, M., Fassett, D., Klopfenstein, J.D., Dinh, D.H., and Rao, J.S. (2010a). Upregulation of PTEN in glioma cells by cord blood mesenchymal stem cells inhibits migration via downregulation of the PI3K/Akt pathway. PLoS One *5*, e10350.

Dasari, V.R., Velpula, K.K., Kaur, K., Fassett, D., Klopfenstein, J.D., Dinh, D.H., Gujrati, M., and Rao, J.S. (2010b). Cord blood stem cell-mediated induction of apoptosis in glioma downregulates X-linked inhibitor of apoptosis protein (XIAP). PLoS One *5*, e11813.

Djouad, F., Plence, P., Bony, C., Tropel, P., Apparailly, F., Sany, J., Noel, D., and Jorgensen, C. (2003). Immunosuppressive effect of mesenchymal stem cells favors tumor growth in allogeneic animals. Blood *102*, 3837-3844.

Einhorn, S., and Grander, D. (1996). Why do so many cancer patients fail to respond to interferon therapy? J Interferon Cytokine Res *16*, 275-281.

Elzaouk, L., Moelling, K., and Pavlovic, J. (2006). Anti-tumor activity of mesenchymal stem cells producing IL-12 in a mouse melanoma model. Exp Dermatol *15*, 865-874.

Faião-Flores, F., Coelho, P., Arruda-Neto, J., and Maria, D.A. (2011). Boron neutron capture therapy induces cell cycle arrest and DNA fragmentation in murine melanoma cells. Appl Radiat Isot *69*, 1741-1744.

Ferlay, J., Soerjomataram, I., Dikshit, R., Eser, S., Mathers, C., Rebelo, M., Parkin, D.M., Forman, D., and Bray, F. (2014). Cancer incidence and mortality worldwide: Sources, methods and major patterns in GLOBOCAN 2012. Int J Cancer.

Freeman, K.P., Hahn, K.A., Harris, F.D., and King, G.K. (2003). Treatment of dogs with oral melanoma by hypofractionated radiation therapy and platinum-based chemotherapy (1987-1997). J Vet Intern Med *17*, 96-101.

Fritz, V., and Jorgensen, C. (2008). Mesenchymal stem cells: an emerging tool for cancer targeting and therapy. Curr Stem Cell Res Ther *3*, 32-42.

Gali-Muhtasib, H., and Bakkar, N. (2002). Modulating cell cycle: current applications and prospects for future drug development. Curr Cancer Drug Targets *2*, 309-336.

Ganta, C., Chiyo, D., Ayuzawa, R., Rachakatla, R., Pyle, M., Andrews, G., Weiss, M., Tamura, M., and Troyer, D. (2009). Rat Umbilical Cord Stem Cells Completely Abolish Rat Mammary Carcinomas with No Evidence of Metastasis or Recurrence 100 Days Post–Tumor Cell Inoculation. Cancer Res *69*, 1815-1820.

Garbe, C., Eigentler, T.K., Keilholz, U., Hauschild, A., and Kirkwood, J.M. (2011). Systematic review of medical treatment in melanoma: current status and future prospects. Oncologist *16*, 5-24.

Garbe, C., McLeod, G.R., and Buettner, P.G. (2000). Time trends of cutaneous melanoma in Queensland, Australia and Central Europe. Cancer *89*, 1269-1278.

Gimble, J., and Guilak, F. (2003). Adipose-derived adult stem cells: isolation, characterization, and differentiation potential. Cytotherapy *5*, 362-369.

Golias, C.H., Charalabopoulos, A., and Charalabopoulos, K. (2004). Cell proliferation and cell cycle control: a mini review. Int J Clin Pract *58*, 1134-1141.

Greenlee, R.T., Murray, T., Bolden, S., and Wingo, P.A. (2000). Cancer statistics, 2000. CA Cancer J Clin *50*, 7-33.

Grosenbaugh, D.A., Leard, A.T., Bergman, P.J., Klein, M.K., Meleo, K., Susaneck, S., Hess, P.R., Jankowski, M.K., Jones, P.D., Leibman, N.F., *et al.* (2011). Safety and efficacy of a xenogeneic DNA vaccine encoding for human tyrosinase as adjunctive treatment for oral malignant melanoma in dogs following surgical excision of the primary tumor. Am J Vet Res *72*, 1631-1638.

Hübner, B., Eckert, K., Garbe, C., and Maurer, H.R. (1995). Synergistic interactions between interferon beta and carboplatin on SK-MEL 28 human

melanoma cell growth inhibition in vitro. J Cancer Res Clin Oncol *121*, 84-88.

Han, Z., Tian, Z., Lv, G., Zhang, L., Jiang, G., Sun, K., Wang, C., Bu, X., Li, R., Shi, Y., *et al.* (2011). Immunosuppressive effect of bone marrow-derived mesenchymal stem cells in inflammatory microenvironment favours the growth of B16 melanoma cells. J Cell Mol Med *15*, 2343-2352.

Herceg, Z., and Wang, Z.-Q. (2001). Functions of poly(ADP-ribose) polymerase (PARP) in DNA repair, genomic integrity and cell death. Mutation Research/Fundamental and Molecular Mechanisms of Mutagenesis *477*, 97-110.

Hong, I.S., Lee, H.Y., and Kang, K.S. (2014). Mesenchymal Stem Cells and Cancer: Friends or Enemies? Mutat Res.

Horikoshi, T., Fukuzawa, K., Hanada, N., Ezoe, K., Eguchi, H., Hamaoka, S., Tsujiya, H., and Tsukamoto, T. (1995). In vitro comparative study of the antitumor effects of human interferon-alpha, beta and gamma on the growth and invasive potential of human melanoma cells. J Dermatol *22*, 631.

Hou, L., Wang, X., Zhou, Y., Ma, H., Wang, Z., He, J., Hu, H., Guan, W., and Ma, Y. (2013). Inhibitory effect and mechanism of mesenchymal stem cells on liver cancer cells. Tumour Biol.
Hou, L., Wang, X., Zhou, Y., Ma, H., Wang, Z., He, J., Hu, H., Guan, W., and Ma, Y. (2014). Inhibitory effect and mechanism of mesenchymal stem cells on liver cancer cells. Tumour Biol *35*, 1239-1250.

Inoue, K., Ohashi, E., Kadosawa, T., Hong, S.H., Matsunaga, S., Mochizuki, M., Nishimura, R., and Sasaki, N. (2004). Establishment and characterization of four canine melanoma cell lines. J Vet Med Sci *66*, 1437-1440.

Jonasch, E., and Haluska, F.G. (2001). Interferon in oncological practice: review of interferon biology, clinical applications, and toxicities. Oncologist *6*, 34-55.

Karimkhani, C., Gonzalez, R., and Dellavalle, R.P. (2014). A Review of Novel Therapies for Melanoma. Am J Clin Dermatol.

Karnoub, A.E., Dash, A.B., Vo, A.P., Sullivan, A., Brooks, M.W., Bell, G.W., Richardson, A.L., Polyak, K., Tubo, R., and Weinberg, R.A. (2007). Mesenchymal stem cells within tumour stroma promote breast cancer metastasis. Nature *449*, 557-563.

Kern, S., Eichler, H., Stoeve, J., Kluter, H., and Bieback, K. (2006). Comparative analysis of mesenchymal stem cells from bone marrow, umbilical cord blood, or adipose tissue. Stem Cells *24*, 1294-1301.

Khakoo, A.Y., Pati, S., Anderson, S.A., Reid, W., Elshal, M.F., Rovira, II, Nguyen, A.T., Malide, D., Combs, C.A., Hall, G., *et al.* (2006). Human mesenchymal stem cells exert potent antitumorigenic effects in a model of Kaposi's sarcoma. J Exp Med *203*, 1235-1247.

Kidd, S., Caldwell, L., Dietrich, M., Samudio, I., Spaeth, E.L., Watson, K., Shi, Y., Abbruzzese, J., Konopleva, M., Andreeff, M., *et al.* (2010). Mesenchymal stromal cells alone or expressing interferon-β suppress pancreatic tumors in vivo, an effect countered by anti-inflammatory treatment. Cytotherapy *12*, 615-625.

Kim, S.K., Kim, S.U., Park, I.H., Bang, J.H., Aboody, K.S., Wang, K.C., Cho, B.K., Kim, M., Menon, L.G., Black, P.M., *et al.* (2006). Human neural stem cells target experimental intracranial medulloblastoma and deliver a therapeutic gene leading to tumor regression. Clin Cancer Res *12*, 5550-5556.

Kirkwood, J.M., and Ernstoff, M.S. (1984). Interferons in the treatment of human cancer. J Clin Oncol *2*, 336-352.

Kitchell, B.E., Brown, D.M., Luck, E.E., Woods, L.L., Orenberg, E.K., and Bloch, D.A. (1994). Intralesional implant for treatment of primary oral malignant melanoma in dogs. J Am Vet Med Assoc *204*, 229-236.

Klopp, A.H., Gupta, A., Spaeth, E., Andreeff, M., and Marini, F., 3rd (2011). Concise review: Dissecting a discrepancy in the literature: do mesenchymal stem cells support or suppress tumor growth? Stem Cells *29*, 11-19.

Komenaka, I., Hoerig, H., and Kaufman, H.L. (2004). Immunotherapy for melanoma. Clin Dermatol *22*, 251-265.

Korn, E.L., Liu, P.Y., Lee, S.J., Chapman, J.A., Niedzwiecki, D., Suman, V.J., Moon, J., Sondak, V.K., Atkins, M.B., Eisenhauer, E.A., *et al.* (2008). Meta-analysis of phase II cooperative group trials in metastatic stage IV melanoma to determine progression-free and overall survival benchmarks for future phase II trials. J Clin Oncol *26*, 527-534.

Lazennec, G., and Jorgensen, C. (2008). Concise review: adult multipotent stromal cells and cancer: risk or benefit? Stem Cells *26*, 1387-1394.

Lee, B., Mukhi, N., and Liu, D. (2012). Current management and novel agents for malignant melanoma. Journal of hematology & oncology *5*, 3.

Lee, M.W., Koh, J.K., Kwon, K.S., Kim, N.I., Kim, S.W., Kim, S.N., Kim, B.S., Kim, Y.C., Kim, J.M., Myung, K.B., *et al.* (2003). Clinical and histopathological study of cutaneous melanoma in Korea. Korean Journal of Dermatology *41*, 43-47.

Li, G.C., Ye, Q.H., Xue, Y.H., Sun, H.J., Zhou, H.J., Ren, N., Jia, H.L., Shi, J., Wu, J.C., Dai, C., *et al.* (2010). Human mesenchymal stem cells inhibit metastasis of a hepatocellular carcinoma model using the MHCC97-H cell line. Cancer Sci *101*, 2546-2553.

Li, H., Fan, X., and Houghton, J. (2007). Tumor microenvironment: the role of the tumor stroma in cancer. J Cell Biochem *101*, 805-815.

Loehrer, P.J., and Einhorn, L.H. (1984). Drugs five years later. Cisplatin. Ann Intern Med *100*, 704-713.

Lu, Y.-r., Yuan, Y., Wang, X.-j., Wei, L.-l., Chen, Y.-n., Cong, C., Li, S.-f., Long, D., Tan, W.-d., Mao, Y.-q., *et al.* (2008). The growth inhibitory effect

of mesenchymal stem cells on tumor cells in vitro and in vivo. Cancer Biol Ther *7*, 245-251.

Maestroni, G.J.M., Hertens, E., and Galli, P. (1999). Factor(s) from nonmacrophage bone marrow stromal cells inhibit Lewis lung carcinoma and B16 melanoma growth in mice. Cell Mol Life Sci *55*, 663-667.

Mansfield, A.S., and Markovic, S.N. (2009). Novel therapeutics for the treatment of metastatic melanoma. Future Oncol *5*, 543-557.

Marino, D.J., Matthiesen, D.T., Stefanacci, J.D., and Moroff, S.D. (1995). Evaluation of dogs with digit masses: 117 cases (1981-1991). J Am Vet Med Assoc *207*, 726-728.

Modiano, J.F., Ritt, M.G., and Wojcieszyn, J. (1999). The molecular basis of canine melanoma: pathogenesis and trends in diagnosis and therapy. J Vet Intern Med *13*, 163-174.

Momin, E.N., Mohyeldin, A., Zaidi, H.A., Vela, G., and Quinones-Hinojosa, A. (2010). Mesenchymal stem cells: new approaches for the treatment of neurological diseases. Curr Stem Cell Res Ther *5*, 326-344.

Moniri, M.R., Sun, X.Y., Rayat, J., Dai, D., Ao, Z., He, Z., Verchere, C.B., Dai, L.J., and Warnock, G.L. (2012). TRAIL-engineered pancreas-derived mesenchymal stem cells: characterization and cytotoxic effects on pancreatic cancer cells. Cancer Gene Ther *19*, 652-658.

Muehlberg, F.L., Song, Y.H., Krohn, A., Pinilla, S.P., Droll, L.H., Leng, X., Seidensticker, M., Ricke, J., Altman, A.M., Devarajan, E., *et al.* (2009). Tissue-resident stem cells promote breast cancer growth and metastasis. Carcinogenesis *30*, 589-597.

Nakamizo, A., Marini, F., Amano, T., Khan, A., Studeny, M., Gumin, J., Chen, J., Hentschel, S., Vecil, G., Dembinski, J., *et al.* (2005). Human bone marrow-derived mesenchymal stem cells in the treatment of gliomas. Cancer Res *65*, 3307-3318.

Nakaya, K., Mizuno, R., and Ohhashi, T. (2001). B16-BL6 melanoma cells release inhibitory factor(s) of active pump activity in isolated lymph vessels. American journal of physiology Cell physiology *281*, C1812-1818.

Neupane, M., Chang, C.C., Kiupel, M., and Yuzbasiyan-Gurkan, V. (2008). Isolation and characterization of canine adipose-derived mesenchymal stem cells. Tissue engineering Part A *14*, 1007-1015.

Ohlsson, L.B., Varas, L., Kjellman, C., Edvardsen, K., and Lindvall, M. (2003). Mesenchymal progenitor cell-mediated inhibition of tumor growth in vivo and in vitro in gelatin matrix. Exp Mol Pathol *75*, 248-255.

Olszanski, A.J. (2014). Current and future roles of targeted therapy and immunotherapy in advanced melanoma. Journal of managed care pharmacy : JMCP *20*, 346-356.

Orbay, H., Tobita, M., and Mizuno, H. (2012). Mesenchymal stem cells isolated from adipose and other tissues: basic biological properties and clinical applications. Stem cells international *2012*, 461718.

Ottnod, J.M., Smedley, R.C., Walshaw, R., Hauptman, J.G., Kiupel, M., and Obradovich, J.E. (2013). A retrospective analysis of the efficacy of Oncept vaccine for the adjunct treatment of canine oral malignant melanoma. Vet Comp Oncol *11*, 219-229.

Ozawa, K., Sato, K., Oh, I., Ozaki, K., Uchibori, R., Obara, Y., Kikuchi, Y., Ito, T., Okada, T., Urabe, M., *et al.* (2008). Cell and gene therapy using mesenchymal stem cells (MSCs). J Autoimmun *30*, 121-127.

Pópulo, H., Soares, P., and Lopes, J.M. (2012). Insights into melanoma: targeting the mTOR pathway for therapeutics. Expert Opin Ther Targets *16*, 689-705.

Pardal, R., Clarke, M.F., and Morrison, S.J. (2003). Applying the principles of stem-cell biology to cancer. Nat Rev Cancer *3*, 895-902.

Parmiani, G., and Colombo, M.P. (1995). Somatic gene therapy of human melanoma: preclinical studies and early clinical trials. Melanoma Res *5*, 295-301.

Proulx, D.R., Ruslander, D.M., Dodge, R.K., Hauck, M.L., Williams, L.E., Horn, B., Price, G.S., and Thrall, D.E. (2003). A retrospective analysis of 140 dogs with oral melanoma treated with external beam radiation. Vet Radiol Ultrasound *44*, 352-359.

Qiao, L., Xu, Z.-l., Zhao, T.-j., Ye, L.-h., and Zhang, X.-d. (2008a). Dkk-1 secreted by mesenchymal stem cells inhibits growth of breast cancer cells via depression of Wnt signalling. Cancer Lett *269*, 67-77.

Qiao, L., Xu, Z., Zhao, T., Zhao, Z., Shi, M., Zhao, R.C., Ye, L., and Zhang, X. (2008b). Suppression of tumorigenesis by human mesenchymal stem cells in a hepatoma model. Cell Res *18*, 500-507.

Quintin-Colonna, F., Devauchelle, P., Fradelizi, D., Mourot, B., Faure, T., Kourilsky, P., Roth, C., and Mehtali, M. (1996). Gene therapy of spontaneous canine melanoma and feline fibrosarcoma by intratumoral administration of histoincompatible cells expressing human interleukin-2. Gene Ther *3*, 1104-1112.

Rachakatla, R.S., Marini, F., Weiss, M.L., Tamura, M., and Troyer, D. (2007). Development of human umbilical cord matrix stem cell-based gene therapy for experimental lung tumors. Cancer Gene Ther *14*, 828-835.

Rassnick, K.M., Ruslander, D.M., Cotter, S.M., Al-Sarraf, R., Bruyette, D.S., Gamblin, R.M., Meleo, K.A., and Moore, A.S. (2001). Use of carboplatin for treatment of dogs with malignant melanoma: 27 cases (1989-2000). J Am Vet Med Assoc *218*, 1444-1448.

Ren, C., Kumar, S., Chanda, D., Kallman, L., Chen, J., Mountz, J.D., and Ponnazhagan, S. (2008). Cancer gene therapy using mesenchymal stem cells expressing interferon-[beta] in a mouse prostate cancer lung metastasis model. Gene Ther *15*, 1446-1453.

Rietschel, P., and Chapman, P.B. (2006). Immunotherapy of melanoma. Hematol Oncol Clin North Am *20*, 751-766.

Rigel, D.S., and Carucci, J.A. (2000). Malignant melanoma: prevention, early detection, and treatment in the 21st century. CA Cancer J Clin *50*, 215-236; quiz 237-240.

Romanov, Y.A., Svintsitskaya, V.A., and Smirnov, V.N. (2003). Searching for alternative sources of postnatal human mesenchymal stem cells: candidate MSC-like cells from umbilical cord. Stem Cells *21*, 105-110.

Roorda, B.D., ter Elst, A., Kamps, W.A., and de Bont, E.S. (2009). Bone marrow-derived cells and tumor growth: contribution of bone marrow-derived cells to tumor micro-environments with special focus on mesenchymal stem cells. Crit Rev Oncol Hematol *69*, 187-198.

Schaffler, A., and Buchler, C. (2007). Concise review: adipose tissue-derived stromal cells--basic and clinical implications for novel cell-based therapies. Stem Cells *25*, 818-827.

Schwarz, P., Withrow, S., Curtis, C., Powers, B., and Straw, R. (1991). Mandibular resection as a treatment for oral cancer in 81 dogs. The Journal of the American Animal Hospital Association (USA).

Secchiero, P., Zorzet, S., Tripodo, C., Corallini, F., Melloni, E., Caruso, L., Bosco, R., Ingrao, S., Zavan, B., and Zauli, G. (2010). Human bone marrow mesenchymal stem cells display anti-cancer activity in SCID mice bearing disseminated non-Hodgkin's lymphoma xenografts. PLoS One *5*, e11140.

Seo, K.W., Lee, H.W., Oh, Y.I., Ahn, J.O., Koh, Y.R., Oh, S.H., Kang, S.K., and Youn, H.Y. (2011a). Anti-tumor effects of canine adipose tissue-derived mesenchymal stromal cell-based interferon-beta gene therapy and cisplatin in a mouse melanoma model. Cytotherapy *13*, 944-955.

Seo, S.H., Kim, K.S., Park, S.H., Suh, Y.S., Kim, S.J., Jeun, S.S., and Sung, Y.C. (2011b). The effects of mesenchymal stem cells injected via different routes on modified IL-12-mediated antitumor activity. Gene Ther *18*, 488-495.

Siegel, R., Naishadham, D., and Jemal, A. (2013). Cancer statistics, 2013. CA Cancer J Clin *63*, 11-30.

Studeny, M., Marini, F., Dembinski, J., Zompetta, C., Cabreira-Hansen, M., Bekele, B., Champlin, R., and Andreeff, M. (2004a). Mesenchymal stem cells: potential precursors for tumor stroma and targeted-delivery vehicles for anticancer agents. J Natl Cancer Inst *96*, 1593 - 1603.
Studeny, M., Marini, F.C., Champlin, R.E., Zompetta, C., Fidler, I.J., and Andreeff, M. (2002). Bone marrow-derived mesenchymal stem cells as vehicles for interferon-beta delivery into tumors. Cancer Res *62*, 3603-3608.

Studeny, M., Marini, F.C., Dembinski, J.L., Zompetta, C., Cabreira-Hansen, M., Bekele, B.N., Champlin, R.E., and Andreeff, M. (2004b). Mesenchymal Stem Cells: Potential Precursors for Tumor Stroma and Targeted-Delivery Vehicles for Anticancer Agents. J Natl Cancer Inst *96*, 1593-1603.

Sun, T., Sun, B.C., Ni, C.S., Zhao, X.L., Wang, X.H., Qie, S., Zhang, D.F., Gu, Q., Qi, H., and Zhao, N. (2008). Pilot study on the interaction between B16 melanoma cell-line and bone-marrow derived mesenchymal stem cells. Cancer Lett *263*, 35-43.

Takahara, K., Ii, M., Inamoto, T., Komura, K., Ibuki, N., Minami, K., Uehara, H., Hirano, H., Nomi, H., Kiyama, S., *et al.* (2014). Adipose-derived stromal cells inhibit prostate cancer cell proliferation inducing apoptosis. Biochem Biophys Res Commun *446*, 1102-1107.

TANG, X.-J., LU, J.-T., TU, H.-J., HUANG, K.-M., FU, R., CAO, G., HUANG, M., CHENG, L.-H., DAI, L.-J., and ZHANG, L. (2014). TRAIL-engineered Bone Marrow-derived Mesenchymal Stem Cells: TRAIL Expression and Cytotoxic Effects on C6 Glioma Cells. Anticancer Res *34*, 729-734.

Thudi, N.K., Martin, C.K., Murahari, S., Shu, S.T., Lanigan, L.G., Werbeck, J.L., Keller, E.T., McCauley, L.K., Pinzone, J.J., and Rosol, T.J. (2011). Dickkopf-1 (DKK-1) stimulated prostate cancer growth and metastasis and inhibited bone formation in osteoblastic bone metastases. Prostate *71*, 615-625.

Todoroff, R.J., and Brodey, R.S. (1979). Oral and pharyngeal neoplasia in the dog: a retrospective survey of 361 cases. J Am Vet Med Assoc *175*, 567-571.

Torsvik, A., and Bjerkvig, R. (2013). Mesenchymal stem cell signaling in cancer progression. Cancer Treat Rev *39*, 180-188.

Uccelli, A., Moretta, L., and Pistoia, V. (2008). Mesenchymal stem cells in health and disease. Nat Rev Immunol *8*, 726-736.

Vaid, M., Prasad, R., Sun, Q., and Katiyar, S.K. (2011). Silymarin targets beta-catenin signaling in blocking migration/invasion of human melanoma cells. PLoS One *6*, e23000.

Wagner, W., Wein, F., Seckinger, A., Frankhauser, M., Wirkner, U., Krause, U., Blake, J., Schwager, C., Eckstein, V., Ansorge, W., *et al.* (2005). Comparative characteristics of mesenchymal stem cells from human bone marrow, adipose tissue, and umbilical cord blood. Exp Hematol *33*, 1402-1416.

Wang, J., Ma, D., Li, Y., Yang, Y., Hu, X., Zhang, W., and Fang, Q. (2014). Targeted delivery of CYP2E1 recombinant adenovirus to malignant melanoma by bone marrow-derived mesenchymal stem cells as vehicles. Anticancer Drugs *25*, 303-314.

Whitley, E.M., Bird, A.C., Zucker, K.E., and Wolfe, L.G. (1995). Modulation by canine interferon-gamma of major histocompatibility complex and tumor-associated antigen expression in canine mammary tumor and melanoma cell lines. Anticancer Res *15*, 923-929.

Wingo, P.A., Ries, L.A., Giovino, G.A., Miller, D.S., Rosenberg, H.M., Shopland, D.R., Thun, M.J., and Edwards, B.K. (1999). Annual report to the nation on the status of cancer, 1973-1996, with a special section on lung cancer and tobacco smoking. J Natl Cancer Inst *91*, 675-690.

Xu, W.T., Bian, Z.Y., Fan, Q.M., Li, G., and Tang, T.T. (2009). Human mesenchymal stem cells (hMSCs) target osteosarcoma and promote its growth and pulmonary metastasis. Cancer Lett *281*, 32-41.

Yan, X.L., Fu, C.J., Chen, L., Qin, J.H., Zeng, Q., Yuan, H.F., Nan, X., Chen, H.X., Zhou, J.N., Lin, Y.L., *et al.* (2012). Mesenchymal stem cells from primary breast cancer tissue promote cancer proliferation and enhance mammosphere formation partially via EGF/EGFR/Akt pathway. Breast Cancer Res Treat *132*, 153-164.

Yang, C., Lei, D., Ouyang, W., Ren, J., Li, H., Hu, J., and Huang, S. (2014). Conditioned media from human adipose tissue-derived mesenchymal stem cells and umbilical cord-derived mesenchymal stem cells efficiently induced the apoptosis and differentiation in human glioma cell lines in vitro. BioMed research international *2014*, 109389.

Yang, M., Ma, Q., Dang, G., Ma, K., Chen, P., and Zhou, C. (2005). In vitro and in vivo induction of bone formation based on ex vivo gene therapy using rat adipose-derived adult stem cells expressing BMP-7. Cytotherapy *7*, 273-281.

Yoo, K.H., Jang, I.K., Lee, M.W., Kim, H.E., Yang, M.S., Eom, Y., Lee, J.E., Kim, Y.J., Yang, S.K., and Jung, H.L. (2009). Comparison of immunomodulatory properties of mesenchymal stem cells derived from adult human tissues. Cell Immunol *259*, 150-156.

Yu, J.M., Jun, E.S., Bae, Y.C., and Jung, J.S. (2008). Mesenchymal stem cells derived from human adipose tissues favor tumor cell growth in vivo. Stem Cells Dev *17*, 463-473.

Zhu, W., Xu, W., Jiang, R., Qian, H., Chen, M., Hu, J., Cao, W., Han, C., and Chen, Y. (2006). Mesenchymal stem cells derived from bone marrow favor tumor cell growth in vivo. Exp Mol Pathol *80*, 267-274.

Zuk, P.A., Zhu, M., Mizuno, H., Huang, J., Futrell, J.W., Katz, A.J., Benhaim, P., Lorenz, H.P., and Hedrick, M.H. (2001). Multilineage cells from human adipose tissue: implications for cell-based therapies. Tissue Eng *7*, 211-228.

국문초록

흑색종 이종이식 마우스모델에서 개와 사람의 지방유래 중간엽줄기세포의 항암효과

안 진 옥

(지도교수 윤 화 영)

서울대학교 대학원

수의학과 수의내과학 전공

중간엽줄기세포는 자기재생과 다분화 기능을 가지고 있어 재생의학과 여러 질환에서 세포치료제로서 사용될 수 있는 잠재적 수단으로 각광받고 있다. 줄기세포는 종양조직으로 이주하는 능력을 가져 항암물질을 종양부위로 전달하는 수송체 기능을 할 수 있다. 따라서 조직재생에 대한 연구와 더불어 종양의 치료에

있어서도 중간엽줄기세포를 이용한 치료는 전도유망한 분야 중 하나이다.

본 논문은 두 단원으로 나누어져 있다. 첫 번째 연구에서는 사람 지방유래 중간엽줄기세포의 흑색종에 대한 항암효과에 대해 다루었다. 생체 외 실험상에서 지방유래 줄기세포의 배양상등액이 A375SM 과 A375P 흑색종 세포주의 증식을 효과적으로 억제하는 것을 MTT 법을 통해 확인하였다. 이러한 결과가 흑색종 세포의 세포주기정지와 세포사멸에 의한 것인지 확인하기 위해 흑색종 세포에 줄기세포의 배양상등액을 72 시간 처리한 후 유세포분석을 실시하였다. 그 결과 줄기세포의 배양상등액이 흑색종 세포의 G_0/G_1 세포주기정지와 세포사멸을 유도하여 흑색종의 증식을 효과적으로 억제함을 확인하였다. Western blot assay 에서 줄기세포 배양상등액을 처리한 흑색종 세포군에서 cyclin D1 단백질의 발현은 감소하였고 caspase-3 와 caspase-7, PARP 의 발현은 증가하였다. 사람의 흑색종을 유발한 마우스 모델에서 줄기세포의 항암효과를 평가하기 위해 CM-DiI 으로 형광 표지한 지방유래 중간엽줄기세포를 마우스에 유발된 종양조직 주변 피하에 주사하고 종양의 크기를 측정하였다. 그 결과 줄기세포가 동물모델에서도 종양의 증식을 억제하였고 종양조직으로 이주한 것을 확인하였다.

두 번째 연구에서는 줄기세포를 이용한 유전자 치료와 저농도의 시스플라틴 항암제를 병용하여 개의 흑색종 치료효과를 확인하고자 하였다. 인터페론 베타를 분비하는 개의 지방유래 중간엽줄기세포가 생체 외 실험상에서 개의 흑색종 세포주의 증식을 억제하였으며, 유세포분석에서 LMeC 의 세포 휴지기의 비율이 증가하고 분열기의 비율은 감소하였다. 이는 인터페론 베타를 분비하는 개의 지방유래 중간엽줄기세포가 흑색종의 세포주기정지를 유도하였음을 지시한다. BALB/c 누드 마우스를 이용한 동물 모델에서 인터페론 베타를 분비하는 개의 지방유래 중간엽줄기세포와 시스플라틴을 병용한 치료군에서 대조군과 단일 치료군에 비해 종양의 증식이 가장 효과적으로 억제되었다. 종양조직에서 TUNEL assay 를 실시하였고, 그 결과 인터페론 베타를 분비하는 개의 지방유래 중간엽줄기세포와 시스플라틴을 병용한 치료군에서 종양의 세포사멸이 유도된 것을 확인하였다.

결론적으로, 본 연구를 통하여 개와 사람의 지방유래 중간엽줄기세포의 흑색종에 대한 항암효과가 증명되었다. 또한 개의 지방유래 중간엽줄기세포는 인터페론 베타를 종양 조직 주변으로 운반하는 세포 수송체로써 효과적으로 이용될 수 있으며, 항암제와 병용 시 항암 효과는 더 극대화될 수 있음을 제시하였다. 따라서 이러한 결과는 앞으로 지방유래 중간엽줄기세포가 새로운

항암 치료제로서 효과적으로 이용될 수 있다는 기초 자료와 과학적 근거로써 활용될 수 있을 것이다.

주 요 어 : 개, 세포 항암치료, 인터페론 베타, 사람, 흑색종, 지방유래 중간엽줄기세포

학 번 : 2011-30491